

# Paleoenvironments of the earliest stone toolmakers, Gona, Ethiopia

Jay Quade<sup>†</sup>

Naomi Levin

Department of Geosciences, University of Arizona, Tucson, Arizona 85721, USA

Sileshi Semaw

Dietrich Stout

Craft Research Center, 419 N. Indian Ave., Indiana University, Bloomington, Indiana 47408, USA

Paul Renne

Berkeley Geochronology Center, 2455 Ridge Rd., Berkeley, California 94709, USA

Michael Rogers

Department of Anthropology, Southern Connecticut State University, 501 Crescent, New Haven, Connecticut 06515-1355, USA

Scott Simpson

Department of Anatomy, School of Medicine, Case Western Reserve University, 10900 Euclid Ave., Cleveland, Ohio 44106-4930, USA

## ABSTRACT

Fluvio-lacustrine sediments of the Hadar and Busidima Formations along the northern Awash River (Ethiopia) archive almost three million years (3.4 to <0.6 Ma) of human evolution, including the earliest documented record of stone toolmaking at 2.5–2.6 Ma. This paper brings together sedimentologic and isotopic evidence for the paleoenvironmental context of early hominids from both formations, but with particular emphasis on the setting for the early toolmakers.

The pre-2.92 Ma record (Hadar Formation) is characterized by low-gradient fluvial, paludal, and lacustrine deposition in an undissected topography most analogous to reaches of the modern middle Awash River near Gewane. The Gona area experienced repeated deep dissection and aggradational by the Awash River, starting between 2.92 and ca. 2.7 Ma and continuing through the top of the record at <0.6 Ma (Busidima Formation). Each aggradational succession is 10–20 m in thickness and fines upward from well-rounded conglomerates at the base to capping paleosols at the top. During this period the ancestral Awash represented by these fining upward sequences was dominantly meandering and flowed northeast, as it does today. Smaller channels tributary to the axial Awash system are also extensively exposed in the Busidima Formation. Compared to the axial-system conglomerates, the tributary

channels transported finer, less mature volcanic clasts mixed with abundant carbonate nodules reworked from adjacent badlands.

Stone artifacts (Oldowan; 2.6–2.0 Ma) at the oldest archaeological sites are only associated with the axial Awash system, in the bedded silts or capping paleosols of the fining upward sequences. The implements were made from rounded cobbles from the channels, but manufacture and use of the tools was always away from the channel bars, on the nearby sandy banks and silt-dominated floodplains. Archaeological sites higher in the record (Acheulian; <1.7 Ma) occur in similar axial river contexts, as well as along tributary channels further removed from artifact raw material sources.

Mature paleosols in the Hadar and Busidima Formations are mostly pale to dark-brown Vertisols typified by abundant clay slickensides, pseudo-anticlinal and vertical fracturing, and carbonate nodules. Such calcic Vertisols are common in the region today, demonstrating that the paleoclimate over the past 3.4 m.y. has been semi-arid and strongly seasonal.

Carbon isotopic results from pedogenic carbonates in the Vertisols allow reconstruction of the proportion of C<sub>3</sub> plants (trees and shrubs) to C<sub>4</sub> plants (grasses) through time. The δ<sup>13</sup>C results from the Hadar Formation prior to 2.9 Ma range from -9.3‰ to -4.1‰, indicating a dominantly forested environment but with locally substantial (average 34%) grasses on the Awash floodplain. The δ<sup>13</sup>C values from soil carbonate in the lower

Busidima Formation (2.7–1.6 Ma) increase (-6.5‰ to -2.7‰) in floodplain paleosols, indicating ~50% average grass cover. Vertisols of the upper Busidima Formation (<1.6 Ma) formed on gently sloping alluvial fans adjacent to the Awash floodplain and display even more positive δ<sup>13</sup>C values, up to -1.8‰, showing that grassland dominated the margins of the active Awash floodplain.

**Keywords:** Gona, Ethiopia, carbon isotopes, early hominids, Oldowan, first stone tools, Awash, paleoenvironment.

## INTRODUCTION

The Hadar Formation, exposed along the northern Awash River (Fig. 1), has been the focus of intense paleoanthropological scrutiny for much of the past several decades. It has yielded a rich array of fossils (e.g., Cooke, 1978; Gentry, 1981; Johanson et al., 1982) including well-known examples of *Australopithecus afarensis* (Johanson and Taieb, 1976; Kimbel et al., 1994). Most research has concentrated on deposits north of the Awash River and east of the Kada Gona River (Fig. 1). Geologic characterization of the Hadar Formation commenced with Taieb et al. (1976), followed by several overview papers (Aronson and Taieb, 1981; Tiercelin, 1986), and studies dealing mainly with geochronology (Aronson et al., 1977; Walter and Aronson, 1982, 1993; Walter, 1994), all largely focused on the lower portion of the Hadar Formation where the *A. afarensis* remains abound. Early researchers

<sup>†</sup>E-mail: jquade@geo.arizona.edu.

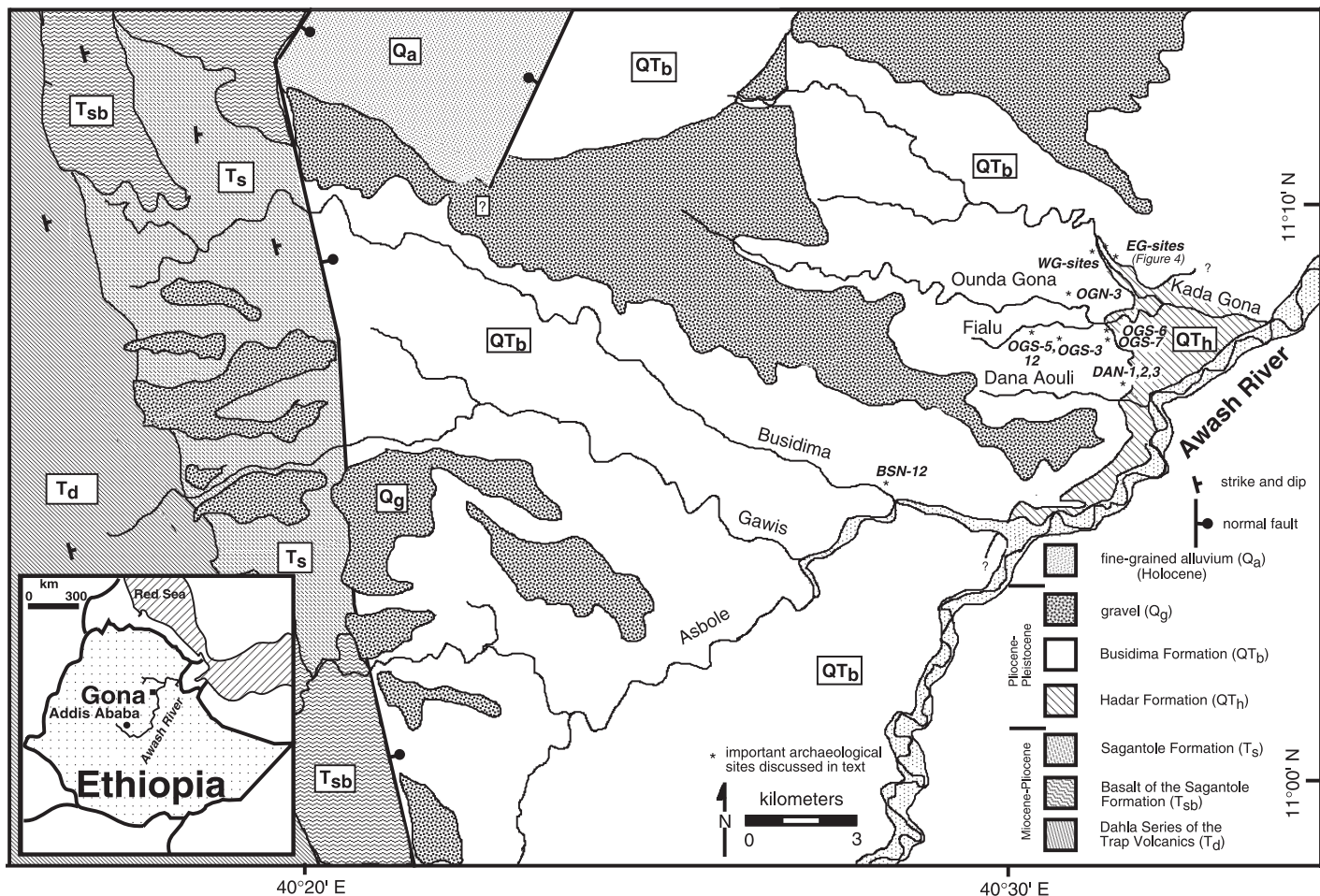


**Figure 1.** Geology and major localities in the Gona project area. Location of Figure 4 panel indicated. The Busidima Formation remains unmapped outside the Gona project area.

also recognized the presence of stone tools low in the section along the Gona River (Roche and Tiercelin, 1977; Corvinus and Roche, 1976), but only recently have these occurrences been firmly placed between 2.5 and 2.6 Ma (Semaw et al., 1997), making them the oldest dated stone implements. The newly designated Busidima Formation (formerly the uppermost Hadar Formation; <2.7 Ma) has been only thinly prospected and documented, although the recent work of Kimbel et al. (1996), Yemane (1997), and Walter et al. (1996) has begun to fill the paleontological and geological gaps.

Our study concentrates on ~120 km<sup>2</sup> of *terra incognita* encompassing the Kada Gona hydrographic basin in the east, and bordered by the Awash River to the southeast, and by the Asbole and Busidima Rivers to the south (Fig. 1). Our characterization of the general geology of this area includes the first detailed geologic map of the deposits, measurement of over 75 stratigraphic sections, physical and geochemi-

cal characterization of the many airfall tuffs exposed in the area, and  $^{40}\text{Ar}/^{39}\text{Ar}$  dates of five phryic tuffs from the largely undated Busidima Formation. These results provide a stratigraphic framework for the rich fossil (including several new hominids) and archaeological remains of the deposits, and for reconstruction of paleoenvironments in the Hadar and Busidima Formations, using carbon isotope results from pedogenic carbonate. Previous efforts to reconstruct paleoenvironments using pollen (Bonnefille et al., 1987) and lacustrine carbonates (Hillaire-Marcel et al., 1982) concentrated almost entirely on the pre-2.6 Ma record. Advances in the use of the stable carbon isotopic composition of paleosol carbonates to reconstruct paleovegetation (Cerling and Quade, 1993) have obvious potential for placing human evolution in the region in a firm paleoenvironmental context. Over seventy isotopic analyses from paleosol carbonates provide the basis for reconstruction of paleovegetation change spanning the period

3.3 to <0.5 Ma along the lower Awash River. The isotopic record of all formations at Gona, with particular emphasis on the oxygen isotope record not discussed here, appears in Levin et al. (2004).

To date, Gona is probably best known for yielding the oldest (2.5–2.6 Ma) documented stone tools in the world (Semaw et al., 1997, 2003). Many have connected stone toolmaking to the emergence of *Homo* sp. in the latest Pliocene. The question many researchers are asking is whether the period of rapid evolutionary change among large mammals (e.g., Vrba, 1995; Feibel, 1999; de Menocal and Bloemberger, 1995; Reed, 1997; Bobe et al., 2002) just prior to the appearance of tools was triggered by changes in the paleoenvironment coincident with global cooling and glaciation. Our evidence from Gona sheds light on the stratigraphic and environmental context of this period of evolutionary change and early toolmaking in the Awash region.

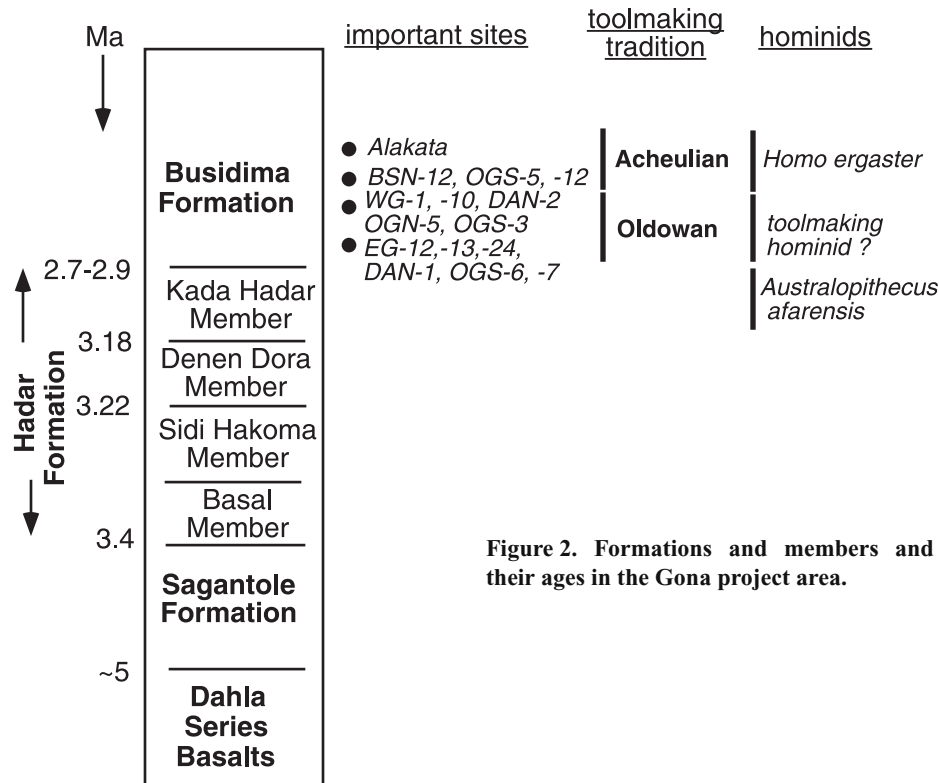


**Figure 2.** Formations and members and their ages in the Gona project area.

### Geologic Setting and Stratigraphic Framework

The Gona project area lies within the Afar sedimentary basin, a structural sub-basin of the Ethiopian Rift bounded to the southeast by the Somalian Escarpment, to the west by the Western Ethiopian Escarpment, and to the north by the Danakil horst. Afar Basin rifting and associated extensive basaltic/trachytic volcanism is thought to have commenced in the early Miocene and continues today (Berhe, 1986; Chernet et al., 1998). Faulting and recent incision by the Awash River have exposed late Tertiary-age deposits over a broad area. The Awash River originates to the south in the Ethiopian highlands and follows the rift north past the project area before turning east and terminating in Lake Abhe.

The Gona project area encompasses several different formations that appear to span much of the last 6 m.y. (Fig. 2). The western part of the area is underlain mainly by basalts intercalated with pockets of fluvio-lacustrine sediment (Fig. 1). The dominantly basaltic portion of these deposits has been mapped as the Dahlia series of the Trap Volcanics and is generally viewed as late Miocene in age (Barberi et al., 1975). The top of this basalt series is locally capped by and/or interfingers with fluvio-lacustrine sediments.

<sup>40</sup>Ar/<sup>39</sup>Ar dating of two tuffs and biostratigraphic

evidence thus far shows that these sediments are late Miocene to early Pliocene in age and therefore overlap with the age of the Sagantole Formation from the middle Awash (Renne et al., 1999; Simpson et al., 2001) (Fig. 2). We have adopted this designation for the deposits in our area. The Sagantole Formation is extensively cut by largely west-dipping normal faults, and is bounded on the east side by a major structural feature, an east-dipping normal fault that we have designated the As Duma Fault. Movement along the As Duma Fault commenced sometime in the early Pliocene, creating the west flank of a structural basin that contains the younger Hadar and Busidima Formations.

The Hadar and Busidima Formations are continuously exposed east of the As Duma Fault (Fig. 1). Depth of dissection increases eastward toward the Awash, and northward. Unlike the Sagantole Formation, the exposed Hadar and Busidima Formations are only slightly deformed or faulted. A minor fault in the lower part of the section was mapped by Tiercelin (1986), and we know of only a few other minor offsets. The Hadar and lower Busidima Formations at Gona are also gently tilted (1–2°) to the west-southwest, based on our theodolite survey of the Gonash-14 (2.53 Ma) tuff.

We follow the member subdivisions for the Hadar Formation, established by Taieb et al. (1976) and firmly dated by later studies. From

bottom to top these are the Basal, Sidi Hakoma, Denen Dora, and Kada Hadar Members. The member boundaries in the Hadar Formation are defined by well-dated marker tuffs rather than by lithologic contrasts, although, as we will discuss below, there is considerable lithologic continuity within members between the Hadar and Gona areas. The lower three members of the Hadar Formation have been described in detail by previous studies (e.g., Tiercelin, 1986; Yemane, 1997) from the Hadar area just to the northeast of Gona, and we will examine them in this paper only briefly.

We propose redesignating the upper part (~80 m thick) of the Kada Hadar Member (Fig. 2) as the Busidima Formation, after the drainage where it is best exposed (Fig. 1). The current stratigraphic scheme reflects the intense paleoanthropological and geochronological scrutiny that the lower ~90 m of the exposed section has enjoyed in the last three decades. By contrast, the upper Kada Hadar Formation (now the Busidima Formation) is >60 m thick and represents four times the duration of the rest of the Hadar Formation, but it remains superficially studied until now. Our proposed change makes geologic sense given the lithologic distinctiveness of the newly designated Busidima Formation, and it will better serve paleoanthropologists as its rich fossil and archaeological story unfolds. Our main focus in this paper will be on the younger artifact-bearing Busidima Formation.

### Hadar Formation

#### *Basal and Sidi Hakoma Members*

The Basal Member is poorly exposed in our project area and was not sampled by us. The contact of the Basal Member and the overlying Sidi Hakoma Member is defined by the Sidi Hakoma Tuff, which is well exposed just east of the confluence of the Kada Gona and Awash Rivers (Fig. 1), a few meters above the Awash floodplain. The Sidi Hakoma Tuff has been correlated with the Tulu Bor Tuff from the Turkana Basin (Brown, 1982) and <sup>40</sup>Ar/<sup>39</sup>Ar dated at 3.40 Ma (Walter and Aronson, 1993). The Sidi Hakoma Member is 40–45 m thick in two sections measured just northeast and southwest of the Kada Gona.

The lower Sidi Hakoma Member consists of fluvial conglomerates and sands interbedded with laminated siltstones and vertic paleosols, which we sampled for isotopic analysis. Dark gray to green laminated mudstone and local limestones rich in fish remains and gastropods (*Melanoides* sp., *Bellamya* sp.) dominate the upper third of the Sidi Hakoma Member in our measured sections, in the same position as similar lacustrine horizons in sections measured

## Composite Stratigraphic Sections

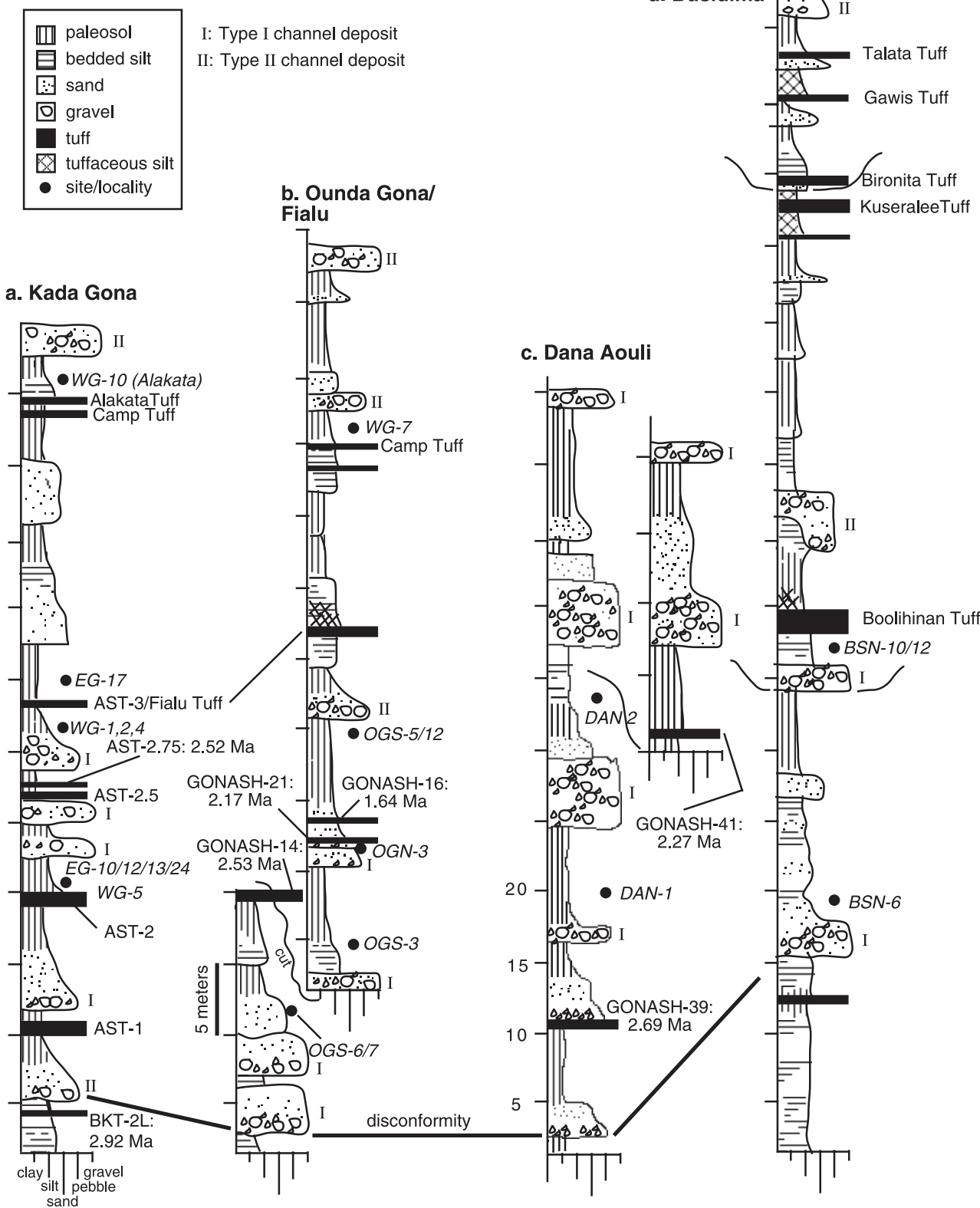


**Figure 3. Composite stratigraphic columns generalizing the stratigraphy of the four (Kada Gona, Ounda Gona/Fialu, Dana Aouli, and Busidima) major areas of exposure (Fig. 1) in the Gona project area.**

by Yemane (1997) to the northeast. A single, dark-brown, 3-m-thick Vertisol occurs near the top of the member; it was sampled in several exposures for isotopic analysis.

#### Denen Dora Member

The base of the Denen Dora Member is defined by the Triple Tuffs,  $^{40}\text{Ar}/^{39}\text{Ar}$  dated to 3.22 Ma (Walter, 1994) in the Hadar area. The tuffs are thin and laterally discontinuous and could not be identified with complete confidence in our measured sections. Thin tuff layers do occur at about the same level in our sections, as described by Yemane (1997), closer to Hadar, which would make the Denen Dora Member 20–24 m thick.

The lower third of the Denen Dora Member consists of gray and green shales containing abundant fish remains and gastropods, and represents a return to lacustrine conditions. The shales grade vertically into a conspicuously dark paleosol with typical vertic features such as slickensides, pseudo-anticlines, and carbonate nodules. The upper half of the Denen Dora

Member consists of ~10 m trough cross-bedded sands and local conglomerate. This sand is well exposed on both banks of the Kada Gona, and is referred to by previous workers (Taieb et al., 1976; Aronson and Taieb, 1981; Tiercelin, 1986) as the DD3 sand. It does not appear to continue far westward into the project area.

#### Kada Hadar Member

The total thickness of the Kada Hadar Member is 20 m along the Ounda Gona and Kada Gona and ~30 m to the southwest, along the Dana Aouli, Busidima/Asbole drainages. The base of the lower Kada Hadar Member is marked by the Kada Hadar Tuff,  $^{40}\text{Ar}/^{39}\text{Ar}$  dated at 3.18 Ma (Walter, 1994). The Kada Hadar Tuff is well exposed in the eastern part of the Gona area and occurs in the base of a paleo-Vertisol developed on top of the DD3 sand. The *A. afaresiensis* fossil Lucy comes from the stratigraphic level just above the Kada Hadar Tuff at Hadar.

Workers at Hadar (e.g., Yemane, 1997) informally subdivided the Kada Hadar into lower

and upper parts, separated by an area-wide disconformity (Aronson et al., 1996; Walter et al., 1996) that is also readily recognizable throughout the Gona area (Figs. 3 and 4). The lower part of the Kada Hadar Member consists of a coarse cobble conglomerate capped by a thick (3–5 m) brown Vertisol complex. These are followed by several minor sand bodies and 5–20 m of thinly bedded siltstone containing gastropods and two laterally traceable green marker beds. The disconformity is cut into this siltstone, which represents the last major lacustrine episode in the area. An anorthoclase-phyric tuff exposed <1 m below the disconformity at Gona yielded a  $^{40}\text{Ar}/^{39}\text{Ar}$  age of  $2.92 \pm 0.006$  Ma and has been correlated with tuff BKT-2L in the Hadar area (Semaw et al., 1997).

#### Busidima Formation

We propose to redesignate that part of the upper Kada Hadar Formation above the area-wide disconformity as the Busidima Formation. The

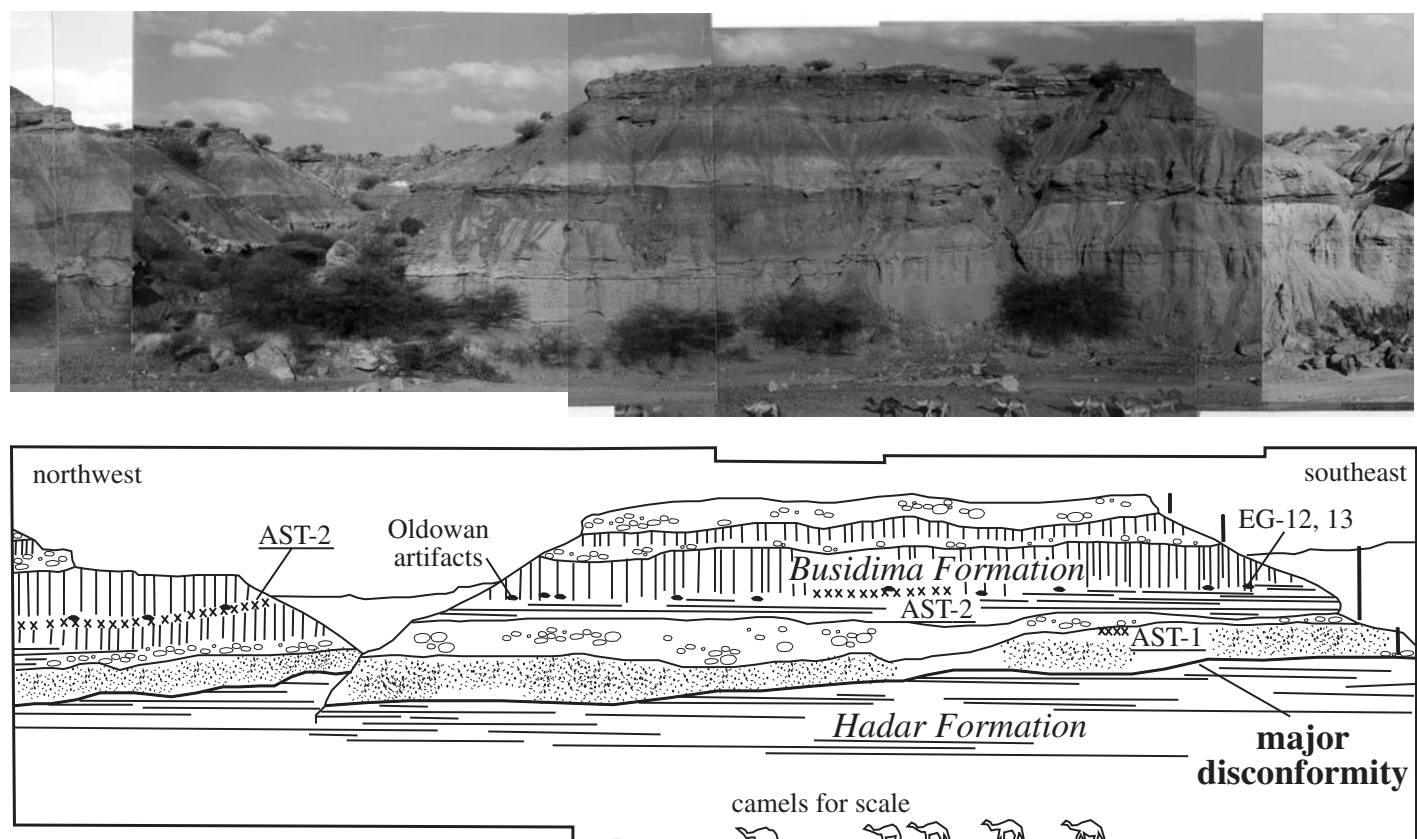


**Figure 4.** Longitudinal profile of the east bank of Kada Gona (see Fig. 1 for location and Fig. 3 for explanation of symbols). The major disconformity dated at 2.9–2.7 Ma marks the boundary between lacustrine siltstone of the uppermost Hadar Formation below and alluvial channel deposits associated with the ancestral Awash River in the Busidima Formation above. The alluvial deposits consist of repeated cycles (extent indicated by solid vertical bars) of well-rounded cobble conglomerates at the base fining upwards into rhizolith-rich sands and paleo-Vertisols at the top. The oldest dated stone implements (2.5–2.6 Ma; Semaw et al., 1997) come from several sites, among them EG-12 and EG-13 indicated, found in the middle of the second fining upward cycle above the disconformity. Marker tuffs AST-1 and AST-2 are also shown. Camels for scale.

new Busidima Formation is a readily mappable (Fig. 1), lithologically distinct unit bounded at its base by an area-wide unconformity representing ~200,000 yr. The type section location and geologic descriptions are provided in the GSA Data Repository.<sup>1</sup> Five newly dated phric tuffs and tephrostratigraphic and fossil evidence from the new Busidima Formation constrain its age between ca. 2.7 and <0.6 Ma (Table 1). By coincidence only, the Busidima Formation encompasses the entire known record of Paleolithic stone tool-making along this reach of the Awash.

The unconformity at the base of the Busidima Formation represents a period of major erosion following the drying of the sub-unconformity lake. Depth of paleo-incision is at least 10 m in some places. This topography was then back-filled with major conglomerate bodies, sands, and floodplain silts. The Gauss-Matuyama boundary (2.58 Ma) has been identified a few meters above the unconformity at Gona (Semaw et al., 1997), and thus aggradation commenced shortly before 2.6 Ma in that area. Aggradation started earlier at Dana Aouli (Fig. 1); there, the unconformity is ~8 m below a newly dated tuff at  $2.69 \pm 0.03$  Ma (Table 1; Fig. 3C). We use this relationship to define the lower age limit of the Busidima Formation at ca. 2.7 Ma. Stone artifacts first appear in the fining upward sequences of these channel fills above the unconformity, the oldest now securely dated at 2.5–2.6 Ma (Semaw et al., 1997, 2002, 2003).

The age of the top of the Busidima Formation is unknown but must be <0.6 Ma. The Bironita Tuff from near the top of the measured section between the Busidima and Gawiis (Fig. 1) can be geochemically correlated with a ca. 0.6 Ma tuff from the middle Awash (Clark et al., 1994; Geraards et al., 2004). Exposures higher in the Busidima Formation south of the Gawiis remain uninvestigated. The Busidima Formation is therefore at least partly equivalent in age to the Wehietu Formation to the south, along the middle Awash (Kalb et al., 1982). The upper Busidima Formation is typified by very mature, stacked Vertisols, locally interbedded with thin channel deposits containing abundant nodules reworked from adjacent paleosols.

We established the stratigraphic context of the fossils, archaeological remains, and paleosol carbonates by measuring and describing seventy-five stratigraphic sections along the Kada Gona, Ounda Gona, Dana Aouli, and Busidima drainages (composite stratigraphy of each area presented in Figures 3A–3D). Correlation of

<sup>1</sup>GSA Data Repository item 2004173, Busidima type section, carbon isotope fractionation, is available on the Web at <http://www.geosociety.org/pubs/ft2004.htm>. Requests may also be sent to editing@geosociety.org.

TABLE 1. SINGLE-CRYSTAL LASER  $^{40}\text{Ar}/^{39}\text{Ar}$  ANALYSES OF TUFF PHENOCRYSTS FROM THE GONA PROJECT AREA

Sample number	Date (Ma) ( $\pm 1\sigma$ )	Number of phenocrysts (crystals)	Location (see Fig. 1)
Gonash-14	$2.534 \pm 0.153$	25	Fialu
Gonash-16	$1.641 \pm 0.014$	14	Fialu
Gonash-21	$2.17 \pm 0.09$	26	Ounda Gona north
Gonash-39	$2.69 \pm 0.03$	17	Dana Aouli
Gonash-41	$2.27 \pm 0.14$	22	Dana Aouli

Note: Tuff samples were wet sieved through the >47 or 63 mesh sizes, and plagioclase or sanidine crystals were handpicked from these mesh fractions for dating.  $^{40}\text{Ar}/^{39}\text{Ar}$  dating of single plagioclase crystals used the methods and facilities described by Renne et al. (1999). Ages are based on co-irradiated Fish Canyon sanidine at 28.02 Ma (Renne et al., 1998), and errors are reported at the  $1\sigma$  level.

beds along each of the drainages was done mainly by tracing key marker tuffs and, in some places, major conglomerate beds. Such physical correlation of beds usually was not possible between major drainages due to the large distances and lack of tuff continuity. In these cases, correlation was achieved largely by dating and by geochemical fingerprinting of tuffs. The main focus of our isotopic sampling in this study was on carbonates from Vertisols within the fining upward sequences. The ages of paleosol carbonates sampled for isotopic analysis were estimated assuming constant sedimentation rates between dated/correlated tephras.

## SEDIMENTOLOGY AND ARCHEOLOGY IN THE BUSIDIMA FORMATION

The lower Busidima Formation at Gona is dominated by a single lithofacies association represented by five to eight fining upward sequences, which are each 5–15 m thick. We follow Miall (1978) in using letter designations of the main lithofacies. A typical association consists of a basal cobble conglomerate (G1) that grades upward into a rhizolith-rich sandstone (S1), capped by bedded siltstone (F), often modified pedogenically at the top. Throughout the text we will refer to these as Type I lithofacies associations. Also present are thinner, less laterally continuous fining upward packages (henceforth Type II lithofacies association) consisting of pebble conglomerate (G2), immature sand usually lacking calcified root remains (S2), and bedded/bioturbated silt (F).

### Lithofacies G

Lithofacies G1 is dominated by clast-supported, massive to crudely stratified (Gm1) coarse cobble conglomerate (Fig. 5A). Average grain size is in the 5–8 cm range, although cobbles >25 cm are locally not uncommon. In general, cobbles are very smooth and rounded to well rounded. Conglomerates can also be

sand-matrix supported, often at the top of the body, and usually are cemented by sparry calcite. Well-developed cross-stratification (Gt1) is uncommon. Conglomerate bodies are sheet-like in geometry, usually traceable for >500 m, and rarely exceed 5 m in thickness.

G1 cobbles are entirely volcanic, and felsic volcanic (rhyolite, trachyte, latite) cobbles consistently dominate over basic volcanic cobbles (largely basalt) (Fig. 6). Most cobbles are porphyritic, with 10%–40% phenocrysts. Aphanitic felsic volcanic clasts are rare but present, in a few cases (<1%) as volcanic cherts. Aphanitic basalt clasts are more common.

We made paleocurrent measurements on 368 imbricated clasts in lithofacies G1 in conglomerates of all ages in the lower Busidima Formation. Paleocurrent directions are dispersed across the northeast quadrant and have an azimuthal vector mean of 40° (Fig. 7). Only westerly and southerly directions are not well represented. The modern Awash River in the Gona and Hadar area also flows east-northeast, but has meander reaches spanning east to north (Fig. 1).

We attribute the deposition of the G1 gravels to the ancestral Awash River, based on the northeasterly paleocurrent directions and physical characteristics. The distinguishing features shared by the G1 gravels and modern Awash River gravel are their coarseness, rounding, lack of micritic carbonate clasts (Fig. 6), and the dominance of porphyritic volcanic clasts. The abundant remains of hippopotamus, crocodile, and aquatic turtle demonstrate that the G1 gravels were deposited by a perennial river, as with the Awash today. This interpretation of the G1 gravels differs from that of Yemane (1997), who viewed them as braided-stream alluvial fan deposits.

Lithofacies G2 is dominated by clast-supported, planar (Gp2) to cross-stratified (Gt2) pebble conglomerate (Fig. 5B). Conglomerate bodies are ribbon-like in geometry, no more than a few tens of meters in cross section but usually hundreds of meters long. Body thickness is highly variable, from <1 m up to ~5 m. Pebbles

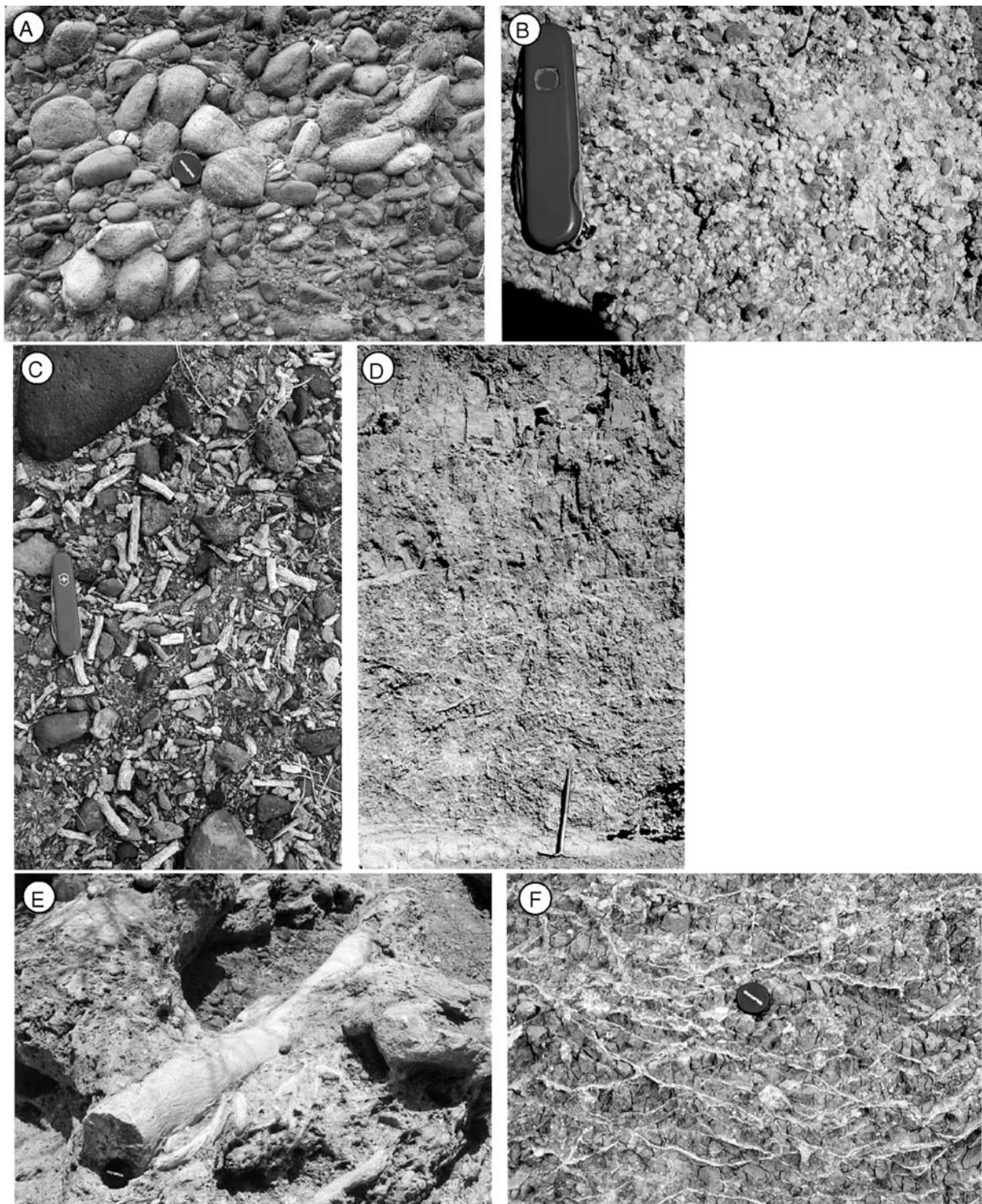


**Figure 5.** (A) Imbricated cobble conglomerates typical of the G1 lithofacies in the lower Busidima Formation. They represent deposition by the ancestral Awash River. Lens cap = 5 cm. (B) Pebble conglomerate rich in reworked paleosol carbonate nodules, typical of the G2 lithofacies deposited by largely ephemeral tributaries to the ancestral Awash, lower Busidima Formation. Knife length = 9 cm. (C) Rhizoliths and other calcified plant remains found commonly in the Sm1 lithofacies, lower Busidima Formation. The rhizoliths formed by calcite replacement of woody stems and roots growing in the paleo-floodplain. Knife length = 9 cm. (D) Complete paleo-Vertisol from the lower Busidima Formation, consisting of a strongly prismatic upper B horizon underlain by a carbonate nodule-rich Bk horizon cut by pseudo-anticlinal fractures. Pick length = 1.1 m. (E) Carbonate pseudomorphic after horizontal tree logs, typical of the Sm1 lithofacies. Lens cap = 5 cm. (F) Detail of Bk horizon from paleosol in Figure 5D showing carbonate nodules and platey carbonate cementation of pseudo-anticlinal fractures. Lens cap = 5 cm.

average 1–2 cm, although fine cobbles (<10 cm) can be abundant in some channels. Pebbles are sub-rounded to sub-angular in the smaller conglomerate bodies up to rounded in the few larger bodies we encountered. Cementation, where present, is by sparry calcite.

G2 pebbles are composed of felsic and basic volcanic clasts mixed in varying proportions (3%–84%) with micritic carbonate clasts. The carbonate clasts are mainly pedogenic nodules reworked from contemporaneous Vertisols. Carbonate clasts tend to dominate the smaller conglomerate bodies. Felsic volcanic clasts dominate over basic volcanic clasts (Fig. 6).

The sharp compositional and textural contrast between lithofacies G1 and G2 indicates that lithofacies G2 was deposited by smaller alluvial systems similar to tributaries to the modern Awash. The relative lack of rounding in G2 gravels points to shorter transport distances. The abundance of micritic carbonate clasts also points to brief transport and derivation from contemporaneously dissected Busidima and Hadar Formation sediments (Figs. 5B and 6). Modern Awash River gravels lack these carbonate clasts, whereas they are ubiquitous in the bedload of the Fialu, Ounda and Kada Gona, and Busidima Rivers once these tributaries enter the Hadar and Busidima Formation badlands (Fig. 6). Clasts in tributaries past and present are dominantly aphanitic, whereas G1 and modern Awash gravels are dominated by porphyritic volcanic rocks. Gravels in modern tributaries consistently show a higher proportion of basic to felsic volcanics than G2 lithofacies in the Busidima Formation. This probably indicates recent exhumation of the late Miocene-age Dahlia Series to the west, which consists of mostly basalt, and through which the larger modern Awash tributaries pass. Most Type II channel deposits lack perennial water fauna, and therefore probably were deposited by ephemeral stream flow. A few Type II deposits in the Busidima Formation have yielded crocodile, marsh cane rat (*Thryonomys swinderianus*), hippopotamus, fish bones and freshwater clams, demonstrating that at least some paleotributaries to the Awash were perennial.

#### Lithofacies S

Lithofacies S1 and S2 both consist of planar stratified (Sp), trough cross-bedded (St), ripple cross-stratified (Sr), and massive (Sm) sand/sandstone. Massive sands are most common toward the top of sand bodies, bedded sands at the base. Sands nearly always fine upwards, from medium to coarse sand at the base to fine sand above. Sand body thicknesses are highly variable, but can reach 2–3 m, especially S1 sands.

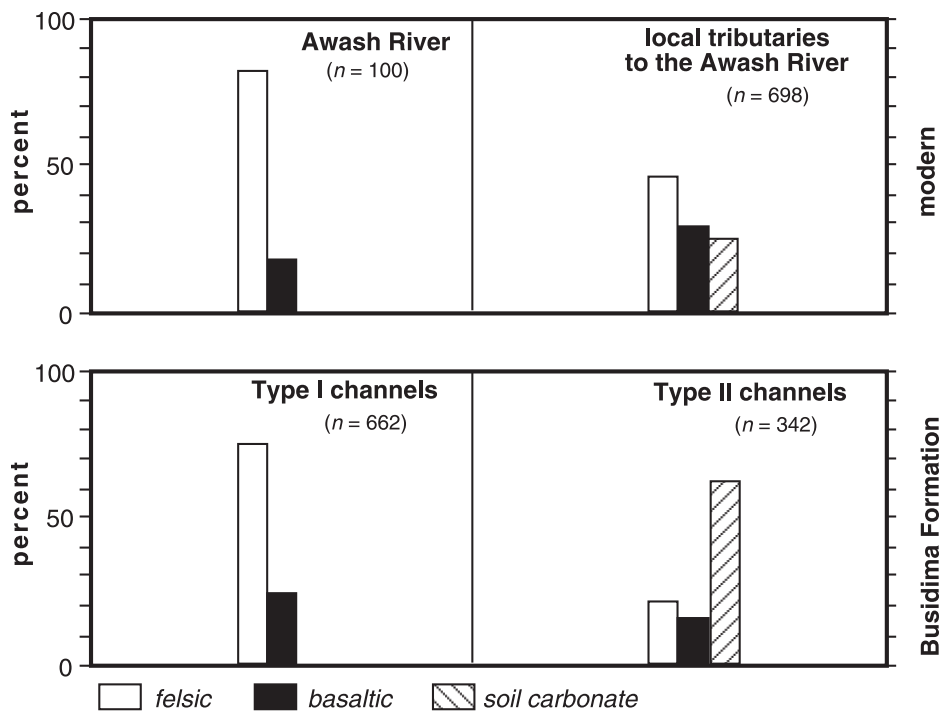


Figure 6. Clast counts in Type I and Type II channels compared with their modern counterparts.

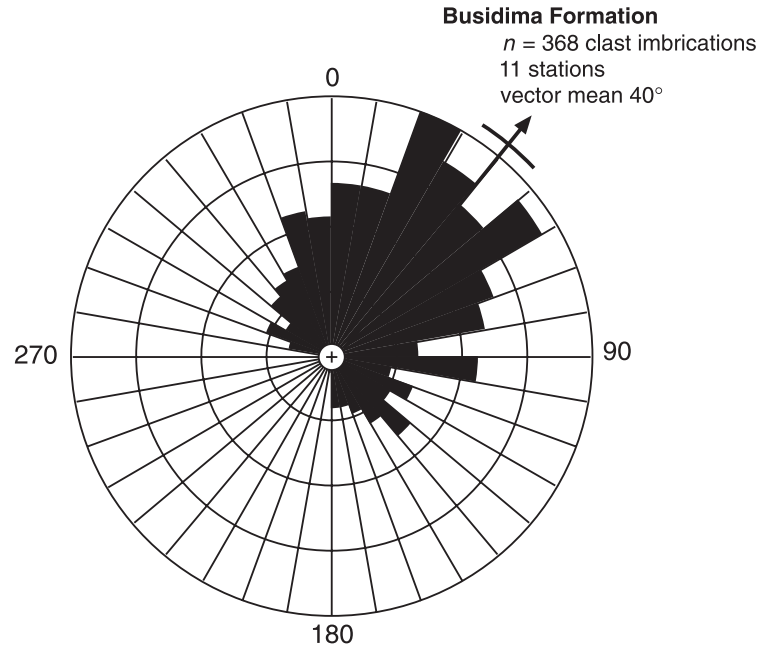
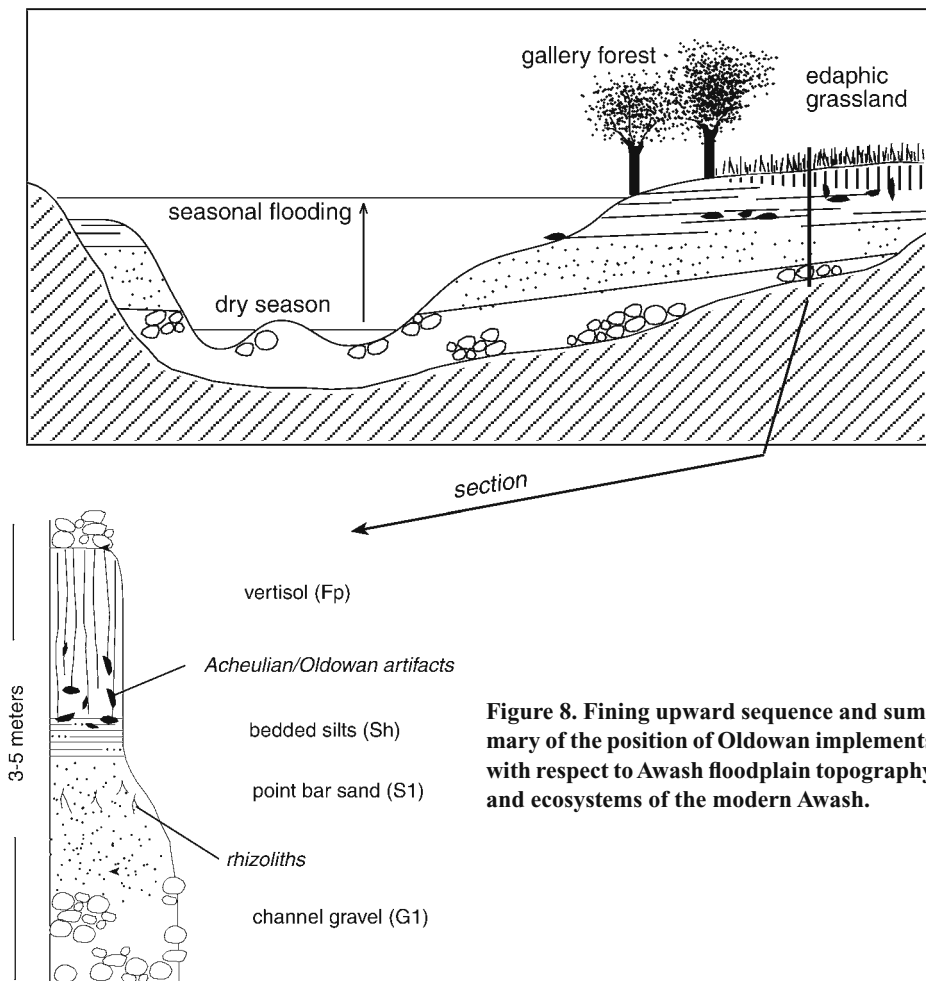


Figure 7. Paleocurrent directions of G1 lithofacies, using pebble imbrications.

Calcified plant remains are nearly ubiquitous in the S1 lithofacies, but are much less common in the S2 lithofacies. They consist of micritic carbonate with some sparry cement, and often preserve a cellular plant structure in thin section.

Many well-preserved examples represent tree logs, roots (rhizoliths), and stumps (Fig. 5E). They vary in diameter between twig-size (4–10 mm) to logs (100–150 mm) (Figs. 5C and 5E). The calicified logs are usually horizontal



**Figure 8. Fining upward sequence and summary of the position of Oldowan implements with respect to Awash floodplain topography and ecosystems of the modern Awash.**

to sub-horizontal (Fig. 5E), whereas the smaller plant remains can be vertical as well.

S1 sands are associated with G1 gravels and S2 with G2. S1 sands differ from S2 in the same way that their associated gravels differ. In particular, S1 sands conspicuously lack grains of reworked pedogenic carbonate, whereas they are abundant in most S2 sands.

#### Lithofacies F

Lithofacies F mainly consists of bedded (Fh), massive (Fm), and pedogenically altered (Fp) mudstone. The bedded mudstone is pale brown (10 YR 7/3-7/4 dry), hard when dry, and locally cemented by flat carbonate nodules. Fm is bioturbated but otherwise unaltered Fh.

Fp consists of slightly darker (10 YR 5/3-4/3 dry) mudstones entirely lacking bedding. The many Fp horizons we examined contain all the classic features of Vertisols (Ahmad, 1983; Lynn and Williams, 1992; Paik and Lee, 1998). Individual peds are angular, blocky and often show slickensides on one or more faces. Single profiles of Fp can reach 3–4 m in thickness and

consist of a prismatic blocky upper zone with dispersed, rounded carbonate nodules and rhizoliths (Fig. 5D). The lower zone is dominated by diagonal fractures that intersect to form pseudo-anticlines (Fig. 5F). Secondary carbonate is abundant as round nodules, rhizoliths, and as plate-shaped cement in the pseudo-anticlinal fractures. The base of Fp is often sharp and marked by a calcified pseudo-anticline, grading downward to Fm over only a few centimeters. Fp horizons capping Type II channel deposits associated with freshwater fauna are conspicuously darker (2.5Y 5/2 dry) than other occurrences, suggesting at least seasonal waterlogging of paleosols.

#### Archaeological Occurrences

There are no identified stone artifacts below the disconformity at the base of the Busidima Formation, even though the appropriate raw materials (of the type used by later toolmakers) are present in at least two gravel bodies prior to 2.9 Ma. One major cobble conglomerate occurs in the lower third of the Sidi Hakoma Member

(ca. 3.3 Ma), and another occurs at the base of the Kada Hadar Member (ca. 3.1 Ma). Large (>20 cm) volcanic cobbles and boulders are locally present in both. Large cobbles in the DD3 sand (ca. 3.2 Ma) can be found but are not common. Extensive survey of the 3.1 Ma conglomerate has not yielded any stone implements. *A. afarensis* was apparently not a stone toolmaker, but not for lack of suitable raw material, which clearly was available at least during some time periods at Gona prior to 2.9 Ma.

Over 14 sites with in situ occurrences of stone tools have been collected or excavated in the Busidima Formation at Gona over the past nine years (Semaw, 2000). Most of these sites contain artifacts typical of the Oldowan stone tool industry, and include unifacially and bifacially flaked cores, flakes, and flaking debris. Of these sites, EG-10, 12, 13, 24, OGS-6, 7 and possibly DAN-1 belong to the period 2.5–2.6 Ma, and WG-1, WG-10, DAN-2, OGS-3, and OGN-5 to the period 2.5–1.9 Ma (Figs. 1 and 3). Several of the sites, such as EG-10 and EG-12, represent locations where early hominids manufactured stone implements from river cobbles, whereas at other sites the nature of hominid activity is unclear (Semaw, 2000).

#### Oldowan Sites

The Oldowan sites occur, without exception, in the middle to upper part of the fining upwards sequences associated with paleo-Awash River deposits (Fig. 8). Two examples, OGS-7 and EG-24, illustrate the two types of artifact occurrences. At OGS-7, the artifacts are flat lying and show no evidence of disturbance by pedogenesis. In contrast, artifacts from EG-24 are often vertically oriented and slightly abraded, consistent with their presence in Vertisols.

OGS-7 lies 7 m below a tuff dated at 2.53 Ma, exposed in steep outcrops along the lower Fialu (Fig. 1; Semaw et al., 2003). The site occurs midway up into the second major fining upward sequence above the disconformity at the base of the Busidima Formation. The base of the channel is filled with several meters of Gm1 gravels typical of axial Awash River deposits. The gravels are capped by rhizolith-rich sands (Sh1 and St1). The artifacts rest directly on Sh1 on the margin of the channel. The sands are overlain by bedded mudstone (Fh) along a sharp, slightly wavy contact. Bioturbation in the sand is confined to a few isolated burrows and root traces. Hundreds of artifacts, mainly flakes, flaking debris, a few cores, and heavily weathered bone fragments were excavated from a 2.6 m<sup>2</sup> area (Semaw et al., 2003). Most flakes were flat lying. The dense clustering and extremely fresh (unabraded, unweathered) appearance of artifacts at this and other sites argue against

reworking of artifacts after site abandonment. Examples of other archaeological sites with fresh, flat-lying artifact occurrences include EG-12 and 13 (Semaw, 2000).

EG-24, located along the Kada Gona, is dated between 2.6 and 2.5 Ma (Semaw, 2000), within the second fining upward sequence above the base of the Busidima Formation (Figs. 1 and 3A). EG-24 lies 4.2 m above a paleo-Awash gravel (Gm1) and 20–30 cm above tuff AST-2. Many of the other Oldowan sites at Kada Gona lie within tuff AST-2. The tuff and overlying mudstone containing EG-24 has undergone extensive pedogenesis, apparent as secondary clay, slickensides, and dispersed carbonate nodules. The artifacts were found dispersed throughout an ~60-cm-thick zone, are often oriented vertically or subvertically, and are slightly worn and polished in appearance. Evidently the intense shrinking, swelling, and cracking typical of Vertisols has dispersed, reoriented, and abraded the artifacts. The near total lack of bone at EG-24, in sharp contrast to the scattered bone found at OGS-7, could be the result of vertical churning and leaching in Vertisols.

The raw materials involved in toolmaking are rounded alluvial cobbles obtained from the axial Awash River deposits. The main rock types involved in toolmaking are aphanitic felsic and basaltic volcanics, rhyolite, trachyte, and latite. The high selectivity for specific clast types by the early hominids at these sites is described in Semaw et al. (1997).

### Acheulian Sites

Archaeological sites containing artifacts of the Acheulian Industrial Complex abound in the project area and are only in the early stages of study. This stone industry is characterized by larger flakes and cores than the Oldowan, and in many sites by large picks and bifacial handaxes. We will focus on just three sites, BSN-12, and OGS-5 and OGS-12, as examples of the two different settings where we have seen Acheulian sites from the lower Busidima Formation.

BSN-12 is located on the east bank of the Busidima River, several hundred meters upstream from its confluence with the Asbole River (Fig. 1). Artifacts have been found in situ at several levels in an ~2 m interval above a major gravel (Gm1) typical of the axial paleo-Awash. The uppermost archaeological horizon is buried by the Boolihinan Tuff (ca. 1.6 Ma?), and a few artifacts have been observed in the tuff itself. The artifacts are typical of the Acheulian in the area, and include several well-made handaxes, although no handaxes have yet been found in situ (Semaw et al., 2001). The tuff itself contained several articulated skeletons of large mammals and a reptile. Their undisturbed state

indicates that the ash fall event probably was the cause of death. The cranial remains of *Homo erectus* (Semaw et al., 2001) were also found eroding from the tuff. The close stratigraphic association of the site with paleo-Awash River gravels shows that the Busidima hominids frequented the paleo-Awash floodplain.

Other Acheulian sites, such as OGS-5 and OGS-12, are associated with small channels tributary to the paleo-Awash, rather than the Awash itself. These sites are located on the Fialu (Fig. 1), at the top of channel deposits containing a tuff dated at 1.64 Ma (Table 1). Numerous large flakes, core tools, and handaxes were found eroding from the top of a channel fill containing a small-pebble gravel (Gm2), mainly of reworked pedogenic carbonate nodules. The carbonate nodules and the small size of the channel indicate that a small, secondary drainage, occupied by a Type II gravel hosts the site. However, the remains of crocodile, freshwater clams and marsh cane rat (*Thryonomys swinderianus*) in the deposits show that the channel was perennial. The closest gravel bodies characteristic of the paleo-Awash (Gm1) occur 11 m downsection and are divided from the Type II channel deposits hosting OGS-5 and OGS-12 by a second Type II channel and two mature Vertisols. OGS-5 and OGS-12 are two of several Acheulian sites located on a Type II channel that suggest expansion of occupation sites away from the main Awash floodplain, in strong contrast to Oldowan site locations. A similar contrast between the distribution of Acheulian and Oldowan sites has also been observed at Koobi Fora in Kenya between Okote Member and KBS Member archaeological sites, respectively (Rogers et al., 1994).

### STABLE ISOTOPIC STUDIES

#### Methods and Theory

Carbonate samples were crushed and roasted under vacuum at 400–450 °C in order to pyrolyze organic matter prior to conversion to CO<sub>2</sub> with 100% phosphoric acid. Isotopic analyses were performed on a Finnigan Delta-S gas-source mass spectrometer at the University of Arizona. Results are presented in the usual delta notation as the per mil (‰) deviation of the sample CO<sub>2</sub> from the PeeDee belemnite (PDB) standard, where  $R = ^{13}\text{C}/^{12}\text{C}$  or  $^{18}\text{O}/^{16}\text{O}$ , and  $\delta = (R_{\text{sample}}/R_{\text{standard}} - 1) \times 1000$ . We used the SV (single vessel) fractionation factor between CO<sub>2</sub> and CaCO<sub>3</sub> of Swart et al. (1991), and Friedman and O’Neil (1977) for standard mean ocean water (SMOW)-PDB conversion. Analytical uncertainties for δ<sup>13</sup>C measurements are <0.1‰ based on repeated measurements of carbonate standards.

The carbon isotopic composition of soil carbonate is determined by the proportions of C<sub>3</sub> and C<sub>4</sub> vegetation growing on the site during pedogenesis and by depth of formation (Cerling, 1984; Quade et al., 1989; Cerling and Quade, 1993). C<sub>3</sub> plants constitute all trees and most shrubs in East Africa, and they average –27.0 ± 1.3‰ in δ<sup>13</sup>C (PDB) values in open-canopy forest, bushland, and savanna in East Africa (Cerling et al., 2003). Virtually all grasses in low to mid-elevation East Africa are C<sub>4</sub> plants, which average –13.3 ± 1.4‰ in δ<sup>13</sup>C from savanna and bushland settings (Cerling et al., 2003). Except where soil respiration rates are low, plant decay and respiration dominate soil CO<sub>2</sub> (Quade et al., 1989). Diffusive transfer of soil CO<sub>2</sub> upward in the soil produces an ~4.4‰ kinetic enrichment in <sup>13</sup>C at steady state, which is observed in a variety of modern soils (Cerling et al., 1991). Soil carbonate forms in isotopic equilibrium with this kinetically enriched CO<sub>2</sub> (Quade et al., 1989; Cerling and Quade, 1993); the equilibrium enrichment factor is 8.9‰ at the local mean annual temperature at Gona of 26 °C. (Romanek et al., 1992). The combination of kinetic and equilibrium fractionation effects should produce a 13.5 ± 0.2‰ enrichment of δ<sup>13</sup>C values in carbonate compared to coexisting, plant-derived soil CO<sub>2</sub> (see GSA Data Repository item for full description of %C<sub>4</sub> biomass estimation from δ<sup>13</sup>C results [see footnote one]).

At shallow depths all soil carbonate is influenced by atmospheric CO<sub>2</sub>. This influence diminishes with soil depth, depending on soil respiration rates. At 50 cm soil depth, soils receiving more than ~50–60 cm of mean annual rainfall are not influenced by atmospheric CO<sub>2</sub> (Quade et al., 1989). Mean annual rainfall in the project area today is ~55 cm/yr. Pollen evidence from the Hadar Formation points to moister conditions in the past (Bonnefille et al., 1987). Thus, we assume that respiration rates have been sufficient to exclude atmospheric CO<sub>2</sub> at the paleosol depths (>50 cm) that we sampled.

A potentially confounding issue for interpreting the isotopic results is the large vertical cracks found in Vertisols that could permit advection of atmospheric CO<sub>2</sub> to deep soil depths. To test this we analyzed carbonate precipitated in the fractures (Fig. 5F, “platey” carbonate) and carbonate nodules found between fractures from single paleo-Vertisol profiles. In two comparisons (Table 2; profiles B and C), the δ<sup>13</sup>C values of nodular and fracture-fill (platey) carbonate overlap. In profile A, the δ<sup>13</sup>C value for nodular carbonate is higher (Table 2; sample GONJQ 89a) than coexisting values from fracture fill (samples GONJQ 86a, 87b, 88a, 88b), the opposite pattern if atmospheric CO<sub>2</sub>

TABLE 2. CARBON ISOTOPIC RESULTS FROM GONA

Sample number	Sample type*	Feature	Age (Ma)	$\delta^{13}\text{C}$ (PDB)	%C <sub>4</sub> <sup>†</sup>
<b>Busidima Formation</b>					
DANL 10	Gravel coating		0.3	-2.85	73
DANL 19	Gravel coating		0.3	-2.48	65
GONJQ253	Gravel coating		0.3	-2.56	68
GONJQ144	Gravel coating		0.3	-1.42	67
GONJQ 62	Gravel coating		0.3	-2.00	76
DANL-101	Gravel coating		0.3	-1.82	86
GONJQ 6a	Gravel coating		0.3	-1.82	73
GONJQ 6b	Gravel coating		0.3	-1.83	86
GONJQ 5a	Nodule		1.1	-5.00	50
GONJQ 83a	Nodule		1.3	-2.60	67
GONJQ 3a	Nodule		1.3	-3.60	60
GONJQ 77a	Nodule		1.35	-3.11	64
GONJQ 78a	Nodule		1.35	-3.50	61
GONJQ 79a	Contact nodule		1.35	-2.40	69
GONJQ 80a	Reworked nodule		1.35	-1.60	74
GONJQ 84a	Nodule		1.35	-5.20	49
GONJQ 2a	Nodule		1.35	-7.00	36
GONJQ112a	Nodule		1.4	-5.46	47
GONJQ109a	S1 rhizolith		1.5	-5.20	49
GONJQ 73a	Nodule		1.5	-5.00	50
GONJQ 66a	Nodule		1.6	-5.90	44
GONJQ 86a	Platey	Paleosol profile A	1.8	-4.90	51
GONJQ 86b	Platey	Paleosol profile A	1.8	-5.70	45
GONJQ 87b	Soil rhizolith	Paleosol profile A	1.8	-4.00	57
GONJQ 88a	Platey	Paleosol profile A	1.8	-4.70	52
GONJQ 88b	Platey	Paleosol profile A	1.8	-5.90	44
GONJQ 89a	Nodule	Paleosol profile A	1.8	-2.70	66
GONJQ 90a	Platey	Paleosol profile B	1.8	-5.10	49
GONJQ 91a	Nodule	Paleosol profile B	1.8	-5.40	47
GONJQ 92a	Nodule	Paleosol profile B	1.8	-4.40	54
GONJQ 93a	Nodule	Paleosol profile B	1.8	-5.80	44
GONJQ 63a	Nodule		2	-4.50	54
GONJQ 95a	Nodule	Paleosol profile C	2	-5.40	47
GONJQ 95b	Nodule	Paleosol profile C	2	-6.40	40
GONJQ 95c	Nodule	Paleosol profile C	2	-4.60	53
GONJQ 96a	Soil rhizolith	Paleosol profile C	2	-5.20	49
GONJQ 96b	Soil rhizolith	Paleosol profile C	2	-4.90	51
GONJQ 97a	Platey	Paleosol profile C	2	-4.10	56
GONJQ 97b	Platey	Paleosol profile C	2	-6.50	39
GONJQ 97c	Platey	Paleosol profile C	2	-6.10	42
GONJQ 99A1	Nodule		2	-4.13	56
GONJQ 99A2	Nodule		2	-4.12	56
GONJQ 99A3	Nodule		2	-4.64	53
GONJQ 99A4	Nodule		2	-4.83	51
GONJQ 13a	Nodule		2.2	-6.36	40
GONJQ 47a	Nodule		2.55	-6.30	41
GonJQ100a	Nodule		2.55	-4.70	52
GONJQ101a	Nodule		2.55	-6.10	42
GONJQ 10a	Nodule		2.55	-3.70	59
GONJQ 11a	Platey		2.55	-4.90	51
GONJQ 46a	S1 rhizolith		2.6	-5.90	44
GONJQ 59a	Nodule		2.6	-6.00	43
GONJQ 7a	Nodule		2.6	-5.60	46
GONJQ 8a	Soil rhizolith		2.6	-5.60	46
GONJQ 9a	Nodule		2.6	-4.80	51
<b>Hadar Formation</b>					
GONJQ 52a	Platey		2.9	-6.49	39
GonJQ 19a	Nodule		2.95	-6.99	36
GONJQ 17A1	Nodule	Nodule A	3.15	-7.87	30
GONJQ 17A10	Nodule	Nodule A	3.15	-7.77	30
GONJQ 17A2	Nodule	Nodule A	3.15	-8.14	28
GONJQ 17A3	Nodule	Nodule A	3.15	-8.19	27
GONJQ 17A4	Nodule	Nodule A	3.15	-7.99	29
GONJQ 17A5	Nodule	Nodule A	3.15	-8.30	26
GONJQ 17A7	Nodule	Nodule A	3.15	-8.66	24
GONJQ 17A9	Nodule	Nodule A	3.15	-8.30	26
GONJQ 17b1	Nodule	Nodule B	3.15	-8.04	28
GONJQ 51a	Nodule		3.16	-9.30	19
GONJQ 21a	Nodule		3.17	-7.40	33
GONJQ 27a	Nodule		3.19	-4.10	56
GONJQ 38a	Nodule		3.2	-4.80	51
GONJQ 49a	Nodule		3.2	-5.00	50
GONJQ 36a	Nodule		3.24	-5.30	48
GONJQ 25a	Nodule		3.25	-6.10	42
GONJQ 26a	Nodule		3.25	-7.70	31
GONJQ 23a	Nodule		3.26	-7.90	29
GONJQ 40a	Nodule		3.26	-6.60	39
GONJQ 31a	Nodule		3.31	-5.33	48

\*Nodule—nODULES FOUND IN PALEO-VERTISOL; PLATEY—PLATE-SHAPED CARBONATE FOUND IN PALEO-VERTISOL FRACTURES; SOIL RHIZOLITH—RHIZOLITH FOUND IN PALEO-VERTISOL; S1 RHIZOLITH—RHIZOLITH FOUND IN S1 (SANDY) LITHOFACIES (SEE TEXT).

<sup>†</sup>Calculated assuming  $\delta^{13}\text{C}$  values (soil carbonate) of -12‰ and +2‰ for pure C<sub>3</sub> and pure C<sub>4</sub> end members, respectively.

influenced the  $\delta^{13}\text{C}$  value of fracture carbonate. Therefore, deep advection of atmospheric CO<sub>2</sub> along fractures is not evident.

Two features suggest that the carbonate preserved in the paleo-Vertisols of the Hadar and Busidima Formations is pedogenic. First, the carbonate in nodules, rhizoliths, and platy carbonate in fracture fill is micritic. Sparry, non-pedogenic carbonate fills thin, millimeter-scale cracks in many nodules, spar that we avoided during sampling. Secondly, reworked micritic nodules are abundant in channel fill (mainly Type II), showing that the micritic carbonate formed prior to channel deposition.

Soil carbonates can be contaminated by detrital carbonate inherited from parent material. The parent material to most paleo-Vertisols in the Hadar and Busidima Formations is floodplain silt. This silt is noncalcareous in Type I channel fill, reflecting the volcanic character of bedrock in the watershed. Type II channels can contain reworked soil carbonate detritus. The matrix surrounding primary carbonate nodules of paleo-Vertisols is usually noncalcareous, suggesting that detrital carbonate was removed by pedogenic leaching prior to soil nodule formation.

## ENVIRONMENTAL SYNTHESIS

Variations in  $\delta^{13}\text{C}$  values across individual soil carbonate nodules (Table 2: nodule 17a: ±0.28‰ [1σ]) and within single profiles (Table 2: profile A: ±1.2‰; profile B: ±0.6‰; profile C: ±0.9‰) are quite small. Thus, at the scale we are sampling the rest of the record (~10 mg subsamples of single nodules), a single analysis should return  $\delta^{13}\text{C}$  values within 1.2‰ (1σ) of other analyses from the same soil. This range is small compared to the large total range of  $\delta^{13}\text{C}$  values (-9.3‰ to -1.6‰) in the record, validating our use of single nodule analyses to reconstruct paleovegetation.

Carbon isotopic results ( $n = 70$ ) from Vertisols indicate that C<sub>4</sub> biomass (grass) ranged from under 10% to over 80% (of plants) in the Kada Hadar and Busidima Formations (Fig. 9; see also Levin et al., 2004). One sigma standard deviations on biomass estimates are ±17%, largely due to the range in  $\delta^{13}\text{C}$  values displayed by East African C<sub>3</sub> and C<sub>4</sub> grasses. In general, the lowest grass percentages from our data are found in Vertisols in the lower half of the Hadar Formation, whereas the highest percentages are associated with Vertisols high in the section that formed on the alluvial flanks of the axial Awash system. We will discuss the isotopic results in three parts following the three major stratigraphic divisions at Gona: (1) a mixed forest and subordinate grassland environment developed around ancestral Awash channels

and at least two paleo-lakes in the Hadar Formation (3.4–2.9 Ma), (2) higher energy fluvial sedimentation by the paleo-Awash River and its tributaries in a more evenly mixed forest/grassland setting in the lower Busidima Formation (2.7 to the Boolihinan Tuff [ca. 1.6 Ma]), and (3) alluvial fan sedimentation in an increasingly grass-dominated landscape, as the main axis of paleo-Awash sedimentation shifted toward the east in the upper Busidima Formation (<1.6 Ma).

### Hadar Formation (3.4–2.9 Ma)

The  $\delta^{13}\text{C}$  values of carbonates from paleo-Vertisols in this period range from  $-9.3\text{\textperthousand}$  to  $-4.1\text{\textperthousand}$ , and average  $-7.0 \pm 1.4\text{\textperthousand}$  ( $n = 24$ ) (Table 2; Fig. 9). This points to 64% average  $\text{C}_3$  plant (trees and shrubs) cover, although the broad range of results (44%–81%) shows that some locations were almost completely forested, whereas others were covered by significant grass in the course of pedogenesis.

This reconstruction matches well with palynological evidence of Bonneville et al. (1987) from samples at Hadar (just east of Gona) spanning 3.4–2.9 Ma. Bonneville et al. (1987) present evidence that the area was covered by montane forest and evergreen bushland now found at moister sites in Ethiopia, over 1000 m above the current elevation of Gona. Our isotopic results are consistent with this, but point to significant and, in a few cases, dominant percentages of  $\text{C}_4$  grasses at all sites. Previous publications have stressed the “forested” habitat of *A. afarensis* (Kimbrel et al., 1996; Reed, 1997). Our results reveal an ecologically mixed (although tree and shrub-dominated) habitat, with a significant grass component.

### Lower Busidima Formation (2.7 Ma to the Boolihinan Tuff)

Our  $\delta^{13}\text{C}$  results point to a modest shift toward greater grass cover in the region, which becomes apparent by 2.7 Ma. The  $\delta^{13}\text{C}$  values of carbonates from the lower Busidima Formation range from  $-6.5\text{\textperthousand}$  to  $-2.7\text{\textperthousand}$  and average  $-5.1 \pm 0.9\text{\textperthousand}$  ( $n = 32$ ) (Table 2; Fig. 9). This average indicates an ~50/50 mix of forest and grasses, with a range of 39%–66% grass cover, contrasted with ~35% average grass cover in the Hadar Formation.

Mammalian fauna from nearby Hadar (Kimbrel et al., 1996) and elsewhere in East Africa (Wesselman, 1995; Bobe et al., 2002) also display a shift from more wet and closed to drier and more open (more grassland) adaptations in the period 3–2.5 Ma. This change coincides with global aridification and cooling associated with the onset of Northern Hemisphere

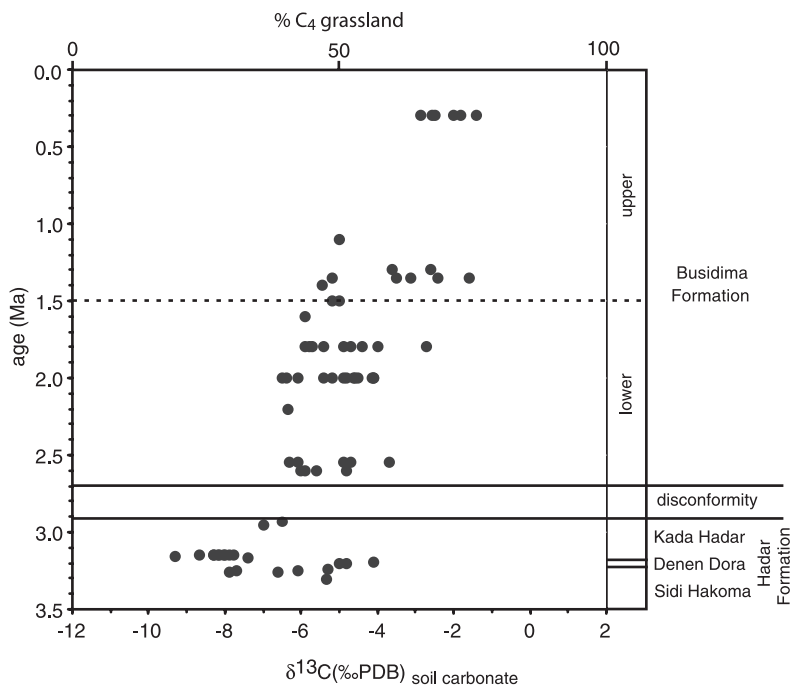


**Figure 9.**  $\delta^{13}\text{C}$  (‰, PeeDee belemnite [PDB]) values of soil carbonate in the Hadar and Busidima Formations (subdivisions shown at right). Percent grassland calculated assuming  $\delta^{13}\text{C}$  values of  $-12\text{\textperthousand}$  and  $+2\text{\textperthousand}$  of soil carbonate associated with end-member  $\text{C}_3$  and  $\text{C}_4$  vegetation, respectively.

glaciation (deMenocal, 1995; deMenocal and Bloemendal, 1995; Dupont and Leroy, 1995). These global and regional changes in turn have been linked to the emergence of *Homo* sp. and associated stone toolmaking. A key point of discussion is how gradual versus “pulsed” or step-like the environmental change was. Elsewhere in East Africa between 2.8 and 2.5 Ma, speciation and extinction in faunal assemblages apparently responded to the expansion of grasslands in pulses rather than gradually (e.g., Vrba, 1995; Bobe et al., 2002). However, there is no evidence from Gona showing that grassland expanded dramatically between 2.9 and 2.5 Ma. Unquestionably, a forest-dominated habitat in the Hadar Formation gave way to a more open environment in the lower Busidima Formation. But from the isotopic perspective, the earliest stone toolmaking at Gona developed in the context of a gradual, not abrupt, grassland expansion that was embedded in a longer term expansion that continued through at least 1.5 Ma.

The record at Gona witnessed a major change in depositional style starting shortly after 2.9 Ma, as the paleo-Awash River incised >10 m, then aggraded with 5–8 fining upward cycles over the next ~1 m.y., depending on location. Explanations for the change in depositional style remain speculative and could be tectonic or climatic. The tectonic explanation entails nor-

mal faulting of the downstream reaches of the Awash, and incision of the river in adjustment to the new lower base level, in the process breaching the Kada Hadar Member lake. The Awash River is cut by numerous east-west-trending normal faults in the area east and north of Hadar before it finally descends into Lake Abhe in the Afar Depression. The Depression only formed in the past 3.5 m.y. (Barberi et al., 1975), but at present too little is known about the timing and roles of tectonic events in that area to offer a good test of the tectonic explanation for paleo-Awash River downcutting. And even if the explanation for incision proves to be tectonic, the effect was transient, as the river began backfilling the low-relief badlands by at least 2.7 Ma, and went on filling the basin with another 80 m of sediment.

Another possible explanation for the change in depositional style is global climate change, in which the onset of glacial climate in the late Pliocene caused the Awash to incise. The main weakness in this explanation is that the Awash River system today displays a whole range of depositional styles, from a deeply incised meandering system in our project area, to a low-energy fluvial to lacustrine system to the south, near Gewane. Tectonic damming by the Bouri horst created the lake there. The extremely active tectonics of the Afar Depression, which

has probably shifted drainages and depocenters throughout the Pliocene and Pleistocene, seems a more plausible explanation for the Awash's change in character near Gona in the late Pliocene. We also speculate that the recent incision by the Awash also must be tectonically related. This is a far more profound event, involving >200 m of downcutting, than the late Pliocene event, which was on the scale of tens of meters. The timing of the onset of incision is not known precisely, but must postdate 0.6 Ma, based on biostratigraphic and tephrostratigraphic evidence from Gona.

The earliest toolmakers appear at Gona shortly after the paleo-Awash River began to aggrade over the disconformity it had created after 2.9 Ma. The earliest post-2.9 Ma aggradation at Gona is represented by a large Type II channel, likely a large tributary to the Awash. No implements have been found with this channel complex, even though it is well exposed and was probably laid down by a perennial river, as indicated by the abundant associated hippopotamus and crocodile remains. The first major Type I gravel to appear in most sections at Kada Gona (the EG-sites), Fialu (OGS-6 and 7), Dana Aouli (DAN-1), and Busidima (BSN-6) has abundant *in situ* artifacts associated with it.

#### Sedimentologic Analogs

Yemane (1997) views the coarse Type I gravels above the disconformity at the base of the Busidima Formation as deposits associated with braided, ephemeral rivers tributary to the paleo-Awash. As noted above, our view is that the Type I gravels are instead associated with the paleo-Awash itself, from evidence that includes north-northeast paleocurrent directions, and cobble rounding and composition. These are all features shared with the modern Awash gravels, but are markedly different from the gravels being carried by modern Awash tributaries.

Given these similarities, we suggest that the modern Awash channel system and floodplain are also a good analog for other sedimentologic features of the lower Busidima Formation, as well as for our isotopic results. The modern Awash next to Gona is deeply incised and narrowly confined to a meander belt-floodplain from 200 to 900 m wide, depending on the reach. The system is dominantly meandering, even though the gradient appears to be large in some reaches (there are no topographic maps of the project area with which to estimate gradient), and even though the river transports small (>25 cm) boulders. Coarse meandering systems today are observed where runoff is strongly seasonal and stream banks are well vegetated (McGowen and Garner, 1970; Gustavson, 1978), as in the Awash today.

Fining upward cycles are conspicuous in the lower Busidima Formation and are consistent with deposition in a meandering system (Fig. 8). These fining upward sequences are similar to ones visible in cut banks of the modern Awash. Well-rounded cobbles compose the basal deposits of the cut-bank exposures, followed by coarse or medium sand (St and Sh) grading upwards to fine sand (Sh, Sr, and Sm). The fine sands are capped by interbedded fine sand and/or silt (Sh or St/Fh) where flooding is recent, or bioturbated sandy silts (Fm) elsewhere, especially on floodplain margins. Fine-grained sediments are in fining upwards packages 10–20 cm thick. Most packages are separated by charred layers that probably represent periodic grass burning by the local Afar people. Other consequences of the periodic flooding are transport of coarse cobbles and fine boulders, which in the dry season are stranded and exposed on side-channel bars, and major destruction of riparian gallery forest, some of which ends up as massive snags of logs, branches, and roots on channel margins. Broken vegetation is common in the cut banks, mainly in the sands (Fig. 10A).

Two features of the fossil fining upward sequences are missing from the modern Awash River deposits: the mature paleosols and calcified plant remains. As previously discussed, the morphology of the calcified plant remains suggests that they are largely pseudomorphic after logs, woody branches and stems, and coarse roots. The size and horizontal orientation of the calcified logs in the sands facies matches with the masses of flood-broken wood in sands of the modern Awash. Replacement of wood by calcite apparently occurs later, after deeper burial. However, the close similarity of the carbon and oxygen isotopic values of the calcified remains and pedogenic carbonate (Table 2) suggests that cementation, although sub-pedogenic, must have occurred shortly after burial, perhaps in the capillary fringe zone (Semeniuk and Meagher, 1981) of the water table, or within the water table itself. The formation of so many tree snags on the modern Awash and those replaced by calcite along the ancestral Awash is and probably was a result of the strongly seasonal pattern of rainfall and flooding in the area.

We did not see any mature soil development in the cut banks of the modern Awash, although weakly developed Vertisols are present on the floodplain margins, furthest from the channel. This is not surprising, given the deep incision of the Awash in the project area. In contrast, the paleo-Awash of the Busidima Formation was less incised and total relief in the badlands along the river was a few tens of meters. A broader floodplain would have meant less frequent flooding of the floodplain margins, and slower

channel migration rates, all permitting more mature Vertisols to develop.

#### Vegetation Analogs

The paleosols that we sampled for isotopic analysis in the lower Busidima Formation are closely associated with paleo-Awash River gravels, inviting some attempt to relate our results to the vegetation distribution in the modern floodplain. There is a consistent pattern to vegetation distribution on the modern floodplain of the Awash. Dense, virtually impenetrable gallery forest grows in a 50–200-m-wide belt along the river (Figs. 10A and 10C–D). We had great difficulty penetrating this vegetation to the riverbanks, except along game trails. Grasses are rare in the forest, except in a few small clearings where sunlight penetrates, and thus we assume that the riparian vegetation is nearly all C<sub>3</sub>. Away from the channel banks, open swards of 1–2-m-high grassland are present, particularly on the inside of meander bends (Figs. 10B and 10C–D). These tall floodplain grasses are probably rooted in the shallow water table and therefore constitute a type of edaphic grassland. Although distinct from the short grasses growing on the broad alluvial flats up and away from the river, all the grasses (short and tall) are C<sub>4</sub> plants.

Using the modern Awash analog, the carbon isotopic results from paleosols indicative of C<sub>3</sub> plants were probably produced by gallery forest and adjacent less dense stands of trees and shrubs on the floodplain. The higher isotopic values indicative of C<sub>4</sub> plants would have been produced largely by edaphic grasses in the meander belt.

The sites chosen for toolmaking by the Oldowan hominids were set in a very regular and specific location in the paleolandscape. Stratigraphically the Oldowan sites are confined to the middle of the fining upward sequences, in bedded sands or in the overlying bedded/bioturbated silts (Fig. 8). No sites have been identified on or in the basal gravels, or at the tops of paleosols high in the fining upward sequences. On the modern Awash this translates into the well-protected, forest-covered banks of the river and the tall edaphic grassland areas beyond, today a narrow band of ground within a few hundred meters of either side of the river. It precludes open channel areas or the depositionally less active areas on the margins or beyond the active floodplain. Moreover, the (as yet) total absence of stone tools in the channel gravels suggests that these early hominids were quarrying their material from the active channels (the only place the cobbles would have been exposed in the channel-floodplain system), but then were systematically transporting the cobbles onto the more protected floodplain to make and use their

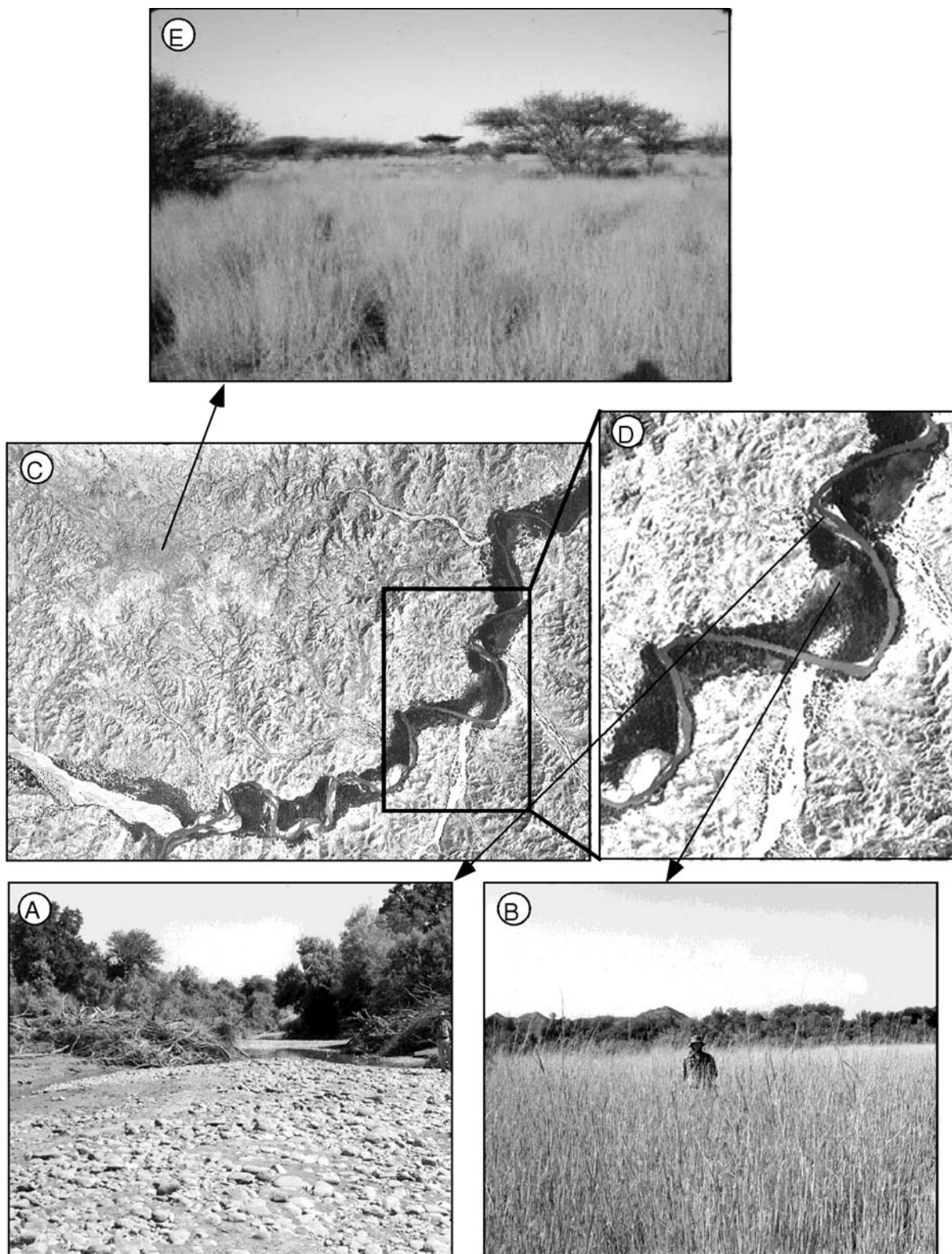


**Figure 10.** (A) Photograph showing an abandoned channel bar and gallery forest bordering the modern Awash River, which serves as an analog for the Type I channel deposits in the lower Busidima Formation. Note the fallen tree snags in sand banks, deposited in recent flooding. Secondary cementation of these produced the calcified plant fragments in Figures 5C and 5E. Location shown in C and D. (B) An open sward of edaphic grassland within a meander bend of the modern Awash River; location shown in C and D. Person for scale. (C and D) Aerial photograph with detail of the Awash River cutting through southern part of the Gona Project area. (E) Savannah developed on mid-Pleistocene gravels at Gona, which serves as a probable modern analog for the paleoenvironment of the upper Busidima Formation.

tools. This is consistent with evidence from the Turkana Basin (Rogers et al., 1994).

### Upper Busidima Formation (above the Boolihinan Tuff)

Sediments above the Boolihinan Tuff (upper Busidima Formation) are dominated by mature Vertisols locally cut by small ephemeral channels (Type II). In our view the sediments were laid down in a distal alluvial fan setting that flanked the axial Awash River system. The  $\delta^{13}\text{C}$  values for soil carbonates from these Vertisols range from  $-7.0\text{\textperthousand}$  to  $-1.8\text{\textperthousand}$ , and average  $-3.8\text{\textperthousand}$  ( $n = 15$ ; Fig. 9). This shows the setting was dominated by  $C_4$  grass ( $\sim 60\%$ ; range 36%–74%). Therefore, the shift toward more grass in the upper part of the section appears to be related to a facies shift as the main Awash drainage migrated to the east, and not necessarily to climate change. This distal alluvial fan setting is extant in the project area west of the Awash (Fig. 10E). It appears as broad plains locally underlain by mature Vertisols and cut by small drainages that head within the immediate area. Vegetation is dominantly  $C_4$  grass (short, non-edaphic), particularly in interfluvial areas, whereas the small drainages are bordered by acacia and assorted  $C_3$  shrubs. This mix is consistent with the  $\delta^{13}\text{C}$  values obtained from soil carbonates above the Boolihinan Tuff.

Archaeologically, the upper Busidima Formation is less rich than deposits lower in the Busidima Formation. We attribute this to the general lack of permanent water in the distal alluvial fan setting. With only a few exceptions so far, Type II channels in the Busidima Formation lack permanent water indicators such as crocodile. Exceptions include the already discussed OGS-5 and OGS-12 along the Ounda Gona (Fig. 3B), Alakata (WG-10) (Fig. 3A), and GAN-10 near the top of the section west of the Busidima (Fig. 3D). The Talalok River, a large perennial tributary to the Awash just south of Gona, is probably a good analog for these settings. These isolated perennial tributary settings are very localized and fossil rich in the Busidima Formation. They may be the context of the “wet and closed” environment reconstructed from faunal evidence in the upper Busidima Formation south of the Asbole (Alemsegid and Geraads, 2000).

### CONCLUDING REMARKS

The Hadar Formation was deposited by a meandering Awash River and several associated lakes. Carbon isotopic evidence shows that the floodplains and lake margins were vegetated

by forest mixed with a locally significant (up to 60%) fraction of edaphic grassland. Between 2.9 and 2.7 Ma, the Awash incised, perhaps because of base-level fall in the Afar Depression, forming an area-wide disconformity. The Awash deposits above the disconformity at the base of the Busidima Formation were coarser than below, but the river system continued to meander, forming distinctive fining upward packages, as it does today.

Within the Busidima Formation, the carbon isotopic evidence collected so far shows a gradual shift toward increasing grass cover through time, but with no apparent abrupt increases in grass abundance on the Awash floodplain as global climate was cooling and drying between 3.0 and 2.5 Ma. Climate was semi-arid and seasonally wet, based on the presence of Vertisols and abundant calcified trees. The first appearance of stone tools at Gona at this time is stratigraphically sudden and environmentally specific. The oldest stone tools are intimately tied to the first occurrence after 3.0 Ma of coarse channel gravels of the paleo-Awash, above a hiatus in the stratigraphy of perhaps 200,000 yr. This pattern suggests that the current estimate of 2.5–2.6 Ma is a *minimum* age for the earliest stone toolmaking in the region, and that the real beginnings of stone toolmaking lie in the 2.6–2.9 Ma period. Early stone toolmaking and use was narrowly confined to the mixed forest and edaphic grassland growing on the paleo-Awash floodplain, unlike later Acheulian toolmakers, who ranged into the secondary drainage systems and perhaps the associated open savannahs with their implements.

Finally, the upper Busidima Formation (ca. 1.6 to  $<0.6$  Ma) was deposited on low-gradient alluvial fans marginal to the ancestral Awash, which by this time had shifted to the east. Carbon isotopic evidence shows the area was covered mainly by grassland, as flat areas marginal to the modern Awash are today.

### ACKNOWLEDGMENTS

We thank K. Schick and N. Toth at the Center for Research into the Archaeological Foundations of Technology (CRAFT) for their crucial support of this project, and Ambacho Kebede, Solomon Kebede, Haptewold Habtemichael, and Yonas Beyene for help with permits. We also thank the Ministry of Youth, Culture, and Sports Affairs of Ethiopia for the field permit, and the assistance of As Mohamed Algani and Mohamed Afkeha from the Education and Culture Bureau of Asyatta. Frank Brown, Yildirim Dilek, Craig Feibel, and Dick Hay all provided excellent feedback on the manuscript. Financial support was provided by the Louis S.B. Leakey Foundation, National Geographic, Wenner-Gren Foundation, and National Science Foundation. Our special thanks to Asahmed Humet and many other Afar tribespeople who in various ways facilitated this research.

### REFERENCES CITED

- Ahmad, N., 1983, Vertisols, in Wilding, L.P., Smeck, N.E., and Hall, G.F., eds., *Pedogenesis and soil taxonomy, II: The soil orders, developments in soil science 11B*: New York, Elsevier, p. 91–123.
- Alemsegid, Z., and Geraads, D., 2000, A new middle Pleistocene fauna from the Busidima-Telalak region of the Afar, Ethiopia: *Comptes Rendus de l'Academie de Sciences de Paris, Sciences de la Terre et Planètes*, v. 331, p. 549–556, doi: 10.1016/S1251-8050(00)01450-6.
- Aronson, J.L., and Taieb, M., 1981, Geology and paleogeography of the Hadar hominid site, Ethiopia, in Rapp, G., and Vondra, C.F., eds., *Hominid sites: Their geologic settings*: Boulder, Colorado, Westview Press, p. 165–195.
- Aronson, J.L., Schmitt, T.J., Walter, R.C., Taieb, M., Tiercelin, J.J., Johanson, D.C., Naeser, C.W., and Nairn, A.E.M., 1977, New geochronologic and paleomagnetic data for the hominid-bearing Hadar Formation of Ethiopia: *Nature*, v. 267, p. 323–327.
- Aronson, J.L., Vondra, C.F., Yemane, T., and Walter, R., 1996, Character of the disconformity in the upper part of the Hadar Formation: Ames, Iowa, Geological Society of America Abstracts with Programs, v. 28, no. 6, p. 28.
- Barberi, F., Ferrara, G., and Santacroce, R., 1975, Structural evolution of the Afar triple junction, in Pilger, A., and Rösler, A., eds., *Afar Depression of Ethiopia*: Stuttgart, West Germany, Schweizerbart, p. 38–54.
- Berhe, S.M., 1986, Geologic and geochronologic constraints on the evolution of the Red Sea–Gulf of Aden and Afar Depression: *Journal of African Earth Sciences*, v. 5, p. 101–117, doi: 10.1016/0899-5362(86)90001-1.
- Bobe, R., Behrensmeyer, A.K., and Chapman, R.E., 2002, Faunal change, environmental variability and late Pliocene hominid evolution: *Journal of Human Evolution*, v. 42, p. 475–497, doi: 10.1006/JHEV.2001.0535.
- Bonnefille, R., Vincens, A., and Buchet, G., 1987, Palynology, stratigraphy and palaeoenvironment of a Pliocene hominid site (2.9–3.3 m.y.) at Hadar, Ethiopia: *Palaeogeography, Palaeoclimatology, Palaeoecology*, v. 60, p. 249–281, doi: 10.1016/0031-0182(87)90035-6.
- Brown, F.H., 1982, Tulu Bor Tuff correlated with Sidi Hakoma Tuff at Hadar: *Nature*, v. 300, p. 631–635.
- Cerling, T.E., 1984, The stable isotopic composition of modern soil carbonate and its relationship to climate: *Earth and Planetary Science Letters*, v. 71, p. 229–240, doi: 10.1016/0012-821X(84)90089-X.
- Cerling, T.E., and Quade, J., 1993, Stable carbon and oxygen isotopes in soil carbonates, in Swart, P., McKenzie, J.A., and Lohmann, K.C., eds., *Continental indicators of climate*, Proceedings of Chapman Conference: Jackson Hole, Wyoming, American Geophysical Union Geophysical Monograph 78, p. 217–231.
- Cerling, T.E., Solomon, D.K., Quade, J., and Bowman, J.R., 1991, On the isotopic composition of carbon in soil carbon dioxide: *Geochimica et Cosmochimica Acta*, v. 55, p. 3403–3405, doi: 10.1016/0016-7037(91)90498-T.
- Cerling, T.E., Harris, J.M., and Passy, B.H., 2003, Diets of East African Bovidae based on stable isotope analysis: *Journal of Mammalogy*, v. 84, no. 2, p. 456–470.
- Chernet, T., Hart, W.K., Aronson, J.L., and Walter, R.C., 1998, New age constraints on the timing of volcanism and tectonism in the northern Main Ethiopian Rift southern Afar transition zone (Ethiopia): *Journal of Volcanology and Geothermal Research*, v. 80, p. 267–280, doi: 10.1016/S0377-0273(97)00035-8.
- Clark, J.D., Beyenne, Y., WoldeGabriel, G., Hart, W.K., Renne, P.R., Gilbert, H., Defleur, A., Suwa, G., Katoh, S., Ludwig, K.R., Bolser, J.-R., Asfaw, B., and White, T.D., 1994, African *Homo erectus*: Old radiometric ages and young Oldowan assemblages in the middle Awash Valley, Ethiopia: *Science*, v. 264, p. 1907–1909.
- Cooke, H.B.S., 1978, Plio-Pleistocene Suidae from Hadar, Ethiopia: *Kirtlandia*, v. 28, p. 1–63.
- Corvinus, G., and Roche, H., 1976, La préhistoire dans la région de Hadar (basin de l'Awash, Afar, Ethiopie): Premiers résultats: *L'Anthropologie*, v. 80, p. 315–324.
- deMenocal, P.B., 1995, Plio-Pleistocene African climate: *Science*, v. 270, p. 53–59.
- deMenocal, P.B., and Bloemendal, J., 1995, Plio-Pleistocene climatic variability in subtropical Africa and the

- paleoenvironment of hominid evolution: A combined data-model approach, in Vrba, E.S., Denton, G.H., Partridge, T.C., and Burckle, L.H., 1995, eds., Paleoclimate and evolution with emphasis on human origins: New Haven, Yale University Press, p. 262–288.
- Dupont, L.M., and Leroy, S.A., 1995, Steps toward drier climatic conditions in northwestern Africa during the Upper Pliocene, in Vrba, E.S., Denton, G.H., Partridge, T.C., and Burckle, L.H., eds., Paleoclimate and evolution with emphasis on human origins: New Haven, Yale University Press, p. 287–298.
- Feibel, C.S., 1999, Basin evolution, sedimentary dynamics, and hominid evolution in East Africa, in Bromage, T.G., and Schrenck, F., eds., African biogeography, climate change, and human evolution: Oxford, Oxford University Press, p. 276–281.
- Friedman, I., and O’Neil, J.R., 1977, Compilation of stable isotope fractionation factors of geochemical interest, in Fleisher, M., ed., Data of geochemistry, chapter KK: U.S. Geological Survey Professional Paper 440-KK, 12 p.
- Gentry, A.W., 1981, Notes on Bovidae (Mammalia) from the Hadar Formation and from Amado and Geraru, Ethiopia: Kirtlandia, v. 33, p. 1–30.
- Geraerts, D., Alemsageged, Z., Reed, D., and Wynn, J., 2004, The Pleistocene fauna from Asbole, lower Awash Valley, Ethiopia, and its environmental and biochronological implications: *Geobios* (in press).
- Gustavson, T.C., 1978, Bed forms and stratification types of modern gravel meander lobes, Nueces River, Texas: *Sedimentology*, v. 25, p. 401–426.
- Hillaire-Marcel, C., Taieb, M., Tiercelin, J.J., and Page, N., 1982, A 1.2-Myr record of isotopic changes in a late Pliocene rift lake, Ethiopia: *Nature*, v. 296, p. 640–642.
- Johanson, D.C., and Taieb, M., 1976, Plio-Pleistocene hominid discoveries in Hadar, Ethiopia: *Nature*, v. 260, p. 293–297.
- Johanson, D.C., Taieb, M., and Coppens, Y., 1982, Pliocene hominids from the Hadar Formation, Ethiopia (1973–1977): Stratigraphic, chronologic, and paleoenvironmental contexts, with notes on hominid morphology and systematics: *American Journal of Physical Anthropology*, v. 57, p. 373–402.
- Kalb, J.E., Oswald, E.B., Tebedge, S., Mebrate, A., Tola, E., and Peak, D., 1982, Geology and stratigraphy of Neogene deposits, middle Awash Valley, Ethiopia: *Nature*, v. 298, p. 17–25.
- Kimbel, W.H., Johanson, D.C., and Rak, Y., 1994, The first skull and other new discoveries of *Australopithecus afarensis*: *Nature*, v. 368, p. 449–451, doi: 10.1038/368449A0.
- Kimbel, W.H., Walter, R.C., Johanson, D.C., Reed, K.E., Aronson, J.L., Assefa, Z., Marean, C.W., Eck, G.G., Bobe, R., Hovers, E., Rak, Y., Vondra, C., Yemane, T., York, D., Chen, Y., Evensen, N.M., and Smith, P.E., 1996, Late Pliocene *Homo* and Oldowan tools from the Hadar Formation (Kada Hadar Member), Ethiopia: *Journal of Human Evolution*, v. 31, p. 549–561, doi: 10.1006/JHEV.1996.0079.
- Levin, N.E., Quade, J., Simpson, S.W., Semaw, S., and Rogers, M., 2004, Isotopic evidence for Plio-Pleistocene environmental change at Gona, Ethiopia: *Earth and Planetary Science Letters*, v. 219, p. 93–110.
- Lynn, W., and Williams, D., 1992, The making of a Vertisol: *Soil Survey Horizons*, v. 33, p. 45–50.
- McGowen, J.H., and Garner, L.E., 1970, Physiographic features and stratification types of coarse-grained point bars: Modern and ancient examples: *Sedimentology*, v. 14, p. 77–111.
- Miall, A.D., 1978, Lithofacies types and vertical profile models in braided river deposits: A summary, in Miall, A.D., ed., *Fluvial sedimentology*: Canadian Society of Petroleum Geology Memoir 5, p. 597–604.
- Paik, I.S., and Lee, Y.I., 1998, Desiccation cracks in vertebral palaeosols of the Cretaceous Hsandong Formation: Genesis and palaeoenvironmental implications: *Sedimentary Geology*, v. 119, p. 161–179, doi: 10.1016/S0037-0738(98)00041-4.
- Quade, J., Cerling, T.E., and Bowman, J.R., 1989, Systematic variation in the carbon and oxygen isotopic composition of Holocene soil carbonate along elevation transects in the southern Great Basin, USA: *Geological Society of America Bulletin*, v. 101, p. 464–475, doi: 10.1130/0016-7606(1989)1012.3.CO;2.
- Reed, K.E., 1997, Early hominid evolution and ecological change through the African Plio-Pleistocene: *Journal of Human Evolution*, v. 32, p. 289–322, doi: 10.1006/JHEV.1996.0106.
- Renne, P.R., Swisher, C.C., Deino, A.L., Karner, D.B., Owens, T., and DePaolo, D.J., 1998, Intercalibration of standards, absolute ages and uncertainties in  $^{40}\text{Ar}/^{39}\text{Ar}$  dating: *Chemical Geology (Isotope Geoscience Section)*, v. 145 (1–2), p. 117–152.
- Renne, P., WoldeGabriel, G., Hart, W.K., Heiken, G., and White, T.D., 1999, Chronostratigraphy of the Mio-Pliocene Sagantole Formation, middle Awash Valley, Afar Rift, Ethiopia: *Geological Society of America Bulletin*, v. 111, p. 869–885, doi: 10.1130/0016-7606(1999)1112.3.CO;2.
- Roche, H., and Tiercelin, J.J., 1977, Decouverte d’industrie lithique ancienne in situ dans la formation d’Hadar, Afar central, Ethiopia: *Comptes Rendus de l’Academie de Paris*, v. 284D, p. 1871–1874.
- Rogers, M.J., Feibel, C.S., and Harris, J.W.K., 1994, Changing patterns of land use by Plio-Pleistocene hominids in the Lake Turkana Basin: *Journal of Human Evolution*, v. 27, p. 139–158, doi: 10.1006/JHEV.1994.1039.
- Romanek, C.S., Grossman, E.T., and Morse, J.W., 1992, Carbon isotopic fractionation in synthetic aragonite and calcite: Effects of temperature and precipitation rate: *Geochimica et Cosmochimica Acta*, v. 56, p. 419–430, doi: 10.1016/0016-7037(92)90142-6.
- Semaw, S., 2000, The world’s oldest stone artifacts from Gona, Ethiopia: Their implications for understanding stone technology and patterns of human evolution between 2.6–1.5 million years ago: *Journal of Archaeological Science*, v. 27, p. 1197–1214, doi: 10.1006/JASC.1999.0592.
- Semaw, S., Renne, P., Harris, J.W.K., Feibel, C.S., Bernor, R.L., Fessaha, N., and Mowbray, K., 1997, 2.5-million-year-old stone tools from Gona, Ethiopia: *Nature*, v. 385, p. 333–335, doi: 10.1038/385333A0.
- Semaw, S., Schick, K., Toth, N., Rogers, M.J., Quade, J., Simpson, S.W., and Dominguez-Rodrigo, M., 2001, Further 2.5–2.6 million year old artifacts, new Plio-Pleistocene archaeological sites and hominid discoveries of 1999 from Gona, Ethiopia: Abstracts for the Paleoanthropology Society Meetings (Kansas City): *Journal of Human Evolution*, v. 40, no. 3, p. A20.
- Semaw, S., Schick, K., Toth, N., Simpson, S., Quade, J., Rogers, M.J., Renne, P., Stout, D., Dominguez-Rodrigo, M., and Hart, W.S., 2002, Recent discoveries from Gona, Afar, Ethiopia: Abstracts for the Paleoanthropology Society Meetings (Denver): *Journal of Human Evolution*, v. 42, no. 3, p. A33.
- Semaw, S., Rogers, M.J., Quade, J., Renne, P., Butler, R.F., Dominguez-Rodrigo, M., Stout, D., Hart, W.S., Pickering, T., and Simpson, S.W., 2003, 2.6-Million-year-old stone tools and associated bones from OGS-6 and OGS-7, Gona, Ethiopia: *Journal of Human Evolution*, v. 45, p. 169–177.
- Semeniuk, V., and Meagher, M.D., 1981, Calcrete in Quaternary coastal dunes in southwestern Australia: A capillary-rise phenomenon associated with plants: *Journal of Sedimentary Petrology*, v. 51, no. 1, p. 47–68.
- Simpson, S., Semaw, S., Schick, K., Toth, N., Quade, J., Dominguez-Rodrigo, M., and Rogers, M.J., 2001, Early Pliocene hominid remains from Gona, Ethiopia: Abstracts for the Paleoanthropology Society Meetings (Kansas City): *Journal of Human Evolution*, v. 40, no. 3, p. A21.
- Swart, P.K., Burns, S.J., and Leder, J.J., 1991, Fractionation of stable isotopes of oxygen and carbon in carbon dioxide during the reaction of calcite with phosphoric acid as a function of temperature and technique: *Chemical Geology*, v. 86, p. 89–96.
- Taieb, M., Johanson, D.C., Coppens, Y., and Aronson, J.L., 1976, Geological and palaeontological background of Hadar hominid site, Afar, Ethiopia: *Nature*, v. 260, p. 289–293.
- Tiercelin, J.J., 1986, The Pliocene Hadar Formation, Afar Depression of Ethiopia, in Frostick, L.E., Renaut, R., Reid, I., and Tiercelin, J.J., eds., *Sedimentation in the African rifts: Geological Society of London Special Publication 23*, p. 221–240.
- Vrba, E., 1995, The fossil record of African antelopes (Mammalia, Bovidae) in relation to human evolution and paleoclimate, in Vrba, E.S., Denton, G.H., Partridge, T.C., and Burckle, L.H., 1995, eds., Paleoclimate and evolution with emphasis on human origins: New Haven, Yale University Press, p. 385–424.
- Walter, R.C., 1994, Age of Lucy and the First Family: Laser  $^{40}\text{Ar}/^{39}\text{Ar}$  dating of the Denen Dora Member of the Hadar Formation: *Geology*, v. 22, p. 6–10, doi: 10.1130/0091-7613(1994)0222.3.CO;2.
- Walter, R.C., and Aronson, J.L., 1982, Revisions of K/Ar ages for the Hadar hominid site, Ethiopia: *Nature*, v. 296, p. 122–127.
- Walter, R.C., and Aronson, J.L., 1993, Age and source of the Sidi Hakoma Tuff, Hadar Formation, Ethiopia: *Journal of Human Evolution*, v. 25, p. 229–240, doi: 10.1006/JHEV.1993.1046.
- Walter, R.C., Aronson, J.L., Chen, Y., Evensen, N., Smith, P.E., and York, D., 1996, New radiometric ages for the Hadar Formation above the disconformity: Ames, Iowa, *Geological Society of America Abstracts with Programs*, v. 28, no. 6, p. 69.
- Wesselman, H.B., 1995, Of mice and almost men: Regional paleoecology and human evolution in the Turkana Basin, in Vrba, E.S., Denton, G.H., Partridge, T.C., and Burckle, L.H., eds., Paleoclimate and evolution with emphasis on human origins: New Haven, Yale University Press, p. 356–368.
- Yemane, T., 1997, Stratigraphy and sedimentology of the Hadar Formation, Afar, Ethiopia [Ph.D. thesis]: Ames, Iowa State University, 182 p.

MANUSCRIPT RECEIVED BY THE SOCIETY 20 MARCH 2003

REVISED MANUSCRIPT RECEIVED 10 DECEMBER 2003

MANUSCRIPT ACCEPTED 31 JANUARY 2004

Printed in the USA